Title
POLARIZATION PHENOMENA IN NUCLEAR REACTIONS

Authors
Glashausser, C.
Thirion, J.

Publication Date
1967-12-01

UCRL-17920

cy. 2

University of California

Ernest O. Lawrence Radiation Laboratory

POLARIZATION PHENOMENA IN NUCLEAR REACTIONS

C. Glashausser and J. Thirion

December 1967

DISCLAIMER

Book Chapter in, "Advances in Nuclear Physics," UCRL-17920

vol. 2, ed. M. Baranger and E. Vogt, Plenum Pub. ~Sept. '68

publication date

UNIVERSITY OF CALIFORNIA

Lawrence Radiation Laboratory
Berkeley, California

AEC Contract No. W-7405-eng-48

POLARIZATION PHENOMENA IN NUCLEAR REACTIONS

C. Glashausser and J. Thirion

December 1967

I. POLARIZED SOURCES

A polarized source is basically an atomic beams apparatus which includes magnetic gradient deflections and high frequency transitions. But the intensities of the neutral beams obtained are much higher than in the devices used in atomic and molecular spectroscopy. The transitions employed are also different; for polarized sources the adiabatic passage method is used to provide high polarization.

1. Sources of Polarized Protons

The general sequence for protons is as follows. The first element in the source is a dissociator which produces hydrogen atoms from molecular hydrogen; it is necessary because the hydrogen molecule has an inconveniently small magnetic moment. The atomic beam is then directed toward a magnet, often a sextupole, designed to produce large magnetic gradients. Here the atoms experience forces which depend on the orientation of the electron spins with respect to the field, just as in the classical Stern-Gerlach experiment. If the spin-up state, for example, is focused to pass through a small exit aperture and the spin-down state rejected, the atomic beam is completely polarized in electronic spins. In the familiar Rabi diagram of Fig. 1, states 1 and 2 are kept; the z-component, m_J, of the spin of essentially all the electrons is then $+1/2$, while the protons are about equally divided into states with $m_I = +1/2$ and $m_I = -1/2$.

There are several ways that the protons could now be polarized, but the method which produces the largest polarization is the adiabatic passage method. Here high-frequency transitions are used to reorient the spins of the protons; two types have been proposed by Abragam and Winter[1] and have

been reviewed in detail by Beurtey.[2] The first can give a proton polarization of +1 by transferring all the atoms in the state 2 to the state 4. A static magnetic field of about 1000 gauss is used; the oscillating electromagnetic field with a frequency of about 3000 Mc is contained in a cavity where 20 watts of high-frequency power are necessary for the transition. The second type is performed in a low magnetic field (about 10 gauss) where F, the spin of the atom, is a good quantum number; the frequency of the oscillating field (about 7 Mc) should then correspond to approximately equal splitting of the F = 1 substates. A proton polarization of -1 is thus achieved by transferring the population of the $m_F = +1$ substate to the substate $m_F = -1$. Note that these high-frequency transitions are useful in polarizing the protons only after the previous separation of electronic spins has been performed; otherwise the exchange of substate populations, partial or complete, would have no effect.

The neutral polarized beam obtained at the exit of the source is then ionized without disturbing the spin state of the nucleus. It has been experimentally verified that the ionization time is much smaller than the period of the Larmor precession of the nucleus, so that the orientation of the nucleus is essentially not modified while the electron is being stripped. Finally, acceleration of the ions should not alter the spin orientations; such depolarization effects can be avoided in tandems and cyclotrons.

The usefulness of a polarized source clearly depends upon the intensity and polarization achieved. Since several reviews[3,4,5] of these sources have been published recently, we shall restrict our discussion to present maximum performance and the factors limiting it.

Limitations

A) Intensity.

Atomic beam intensities of 10^{17} atoms/sec over an area of 0.5 cm^2 have been obtained at Saclay after the magnetic separation. This is the maximum observed thus far. Two factors limit this intensity. The first is the production of the beam in a given solid angle. The dissociation of the hydrogen molecules is performed at a pressure[6] of 2 mm of Hg and the beam is formed by an arrangement of apertures similar to the ones studied by Becker[7] at higher pressures for supersonic flow. In the present application higher pressures of hydrogen cannot be used because of the rapid recombination rate of atomic hydrogen at room temperature. Of course high temperatures could induce dissociation, but the increased velocity of the atoms would be a drawback both for magnetic-gradient focusing and ionization efficiency. The second limitation is the residual pressure in the region near the axis of the sextupole magnet which introduces an attenuation of the atomic beam by scattering. The pumping speed there is limited by the geometry of the unavoidable pole pieces of the sextupole magnet. Both factors give about the same limit, so that both must be improved at the same time to obtain increased beams.

The neutral atoms are ionized[8] in collisions with electrons confined in the magnetic field of a solenoid. Here the limit is probably due to space charge effects. One is concerned not only with ionization efficiency but also with the quality of the ionized beam, its emittance and energy-spread. The quality has to match the acceptance of the accelerator itself.

A polarized proton beam of 6 μA has been obtained at Saclay with a quality suitable for injection into the cyclotron. The trochoidal method[9] is then used to inject the particles into the center of the cyclotron along the median plane. Extracted beams up to about 35 nA have been obtained.[10] This value can certainly be increased by bunching[11] the beam at injection to match the phase acceptance of the machine.

B) Polarization.

The efficiency of the low field transitions is known[12] to be 99.5 ± 0.5%, so that the protons in the atomic beam are completely polarized. Departures from the maximum arise from conditions at the ionizer. Here there is a 5 - 15% background of unpolarized protons arising from two sources. The first is the hydrogen, mostly in the form of H_2O, in the residual vacuum; this can be minimized by liquid air traps, e.g. The second is that part of the hydrogen of the atomic beam itself which is depolarized by scattering in the ionization volume; it is a small factor if the pumping is carefully designed. Depolarizing effects can arise here also due to the state mixing of the hydrogen atom in the magnetic field at the ionizer; it decreases as the field increases and is calculated to be typically between 2 - 5%. The polarization of the ionized protons is thus generally of the order of 80 - 90% in such sources.

2. Deuterons

The description of the polarization parameters for deuterons is considerably more complicated than for protons. The notation that we shall use is that of Raynal[13]; it corresponds to a special choice of irreducible tensor operator T, which gives the following decomposition of the density matrix ρ:

$$\rho = \frac{1}{3} \sum_{\lambda,\mu} \rho_{\lambda,\mu} T_{\lambda,\mu} \qquad (1)$$

Explicitly,

$$\rho = \frac{1}{3} \begin{vmatrix} 1 + \sqrt{\frac{3}{2}}\,\rho_{1,0} + \sqrt{\frac{1}{2}}\,\rho_{2,0} & \sqrt{\frac{3}{2}}\,(\rho_{1,-1} + \rho_{2,-1}) & \sqrt{3}\,\rho_{2,-2} \\ \sqrt{\frac{3}{2}}\,(\rho_{1,1} + \rho_{2,1}) & 1 - \sqrt{2}\,\rho_{2,0} & \sqrt{\frac{3}{2}}\,(\rho_{1,-1} - \rho_{2,-1}) \\ \sqrt{3}\,\rho_{2,2} & \sqrt{\frac{3}{2}}\,(\rho_{1,1} - \rho_{2,1}) & 1 - \sqrt{\frac{3}{2}}\,\rho_{1,0} + \sqrt{\frac{1}{2}}\,\rho_{2,0} \end{vmatrix} \qquad (2)$$

The parameters $\rho_{1,\mu}$ are the vector polarization parameters; the $\rho_{2,\mu}$ are the tensor polarization parameters.

The correspondence between the operator T and the operators which have been used by some other authors[14] is as follows:

$$\begin{aligned} T_{1,0} &= \sqrt{\tfrac{3}{2}}\, S_z \\ T_{1,\pm 1} &= \sqrt{\tfrac{3}{2}}\,(\mp S_{\pm}) = \sqrt{\tfrac{3}{2}}\,(\mp S_x - iS_y) \\ T_{2,0} &= \frac{3}{\sqrt{2}}\, S_{zz} \\ T_{2,\pm 1} &= \sqrt{3}\,(\mp S_{zx} - iS_{zy}) \\ T_{2,\pm 2} &= \frac{\sqrt{3}}{2}\,(S_{xx} - S_{yy} \pm 2S_{xy}) \end{aligned} \qquad (3)$$

The properties of the polarized sources described here are such that the density matrix ρ of the polarized beam is diagonal, with the z axis taken as the direction of the magnetic field at the ionizer. There are six allowed

sets of parameter values, corresponding to two thirds of the deuterons in one magnetic substate (1, 0, or -1) and one third in one of the other two substates. The allowed density matrix elements are thus:

$$\rho_{1,0} = \pm\sqrt{\frac{2}{3}},\ \rho_{20} = 0;$$
$$\rho_{1,0} = \pm\sqrt{\frac{1}{6}},\ \rho_{20} = \pm\sqrt{\frac{1}{2}} \quad . \tag{4}$$

The first two sets correspond to a pure vector polarized beam (all the $\rho_{2,\mu}$ are zero). If we choose the positive sign for $\rho_{1,0}$, the density matrix is, according to Eq. (2),

$$\rho = \frac{1}{3}\begin{vmatrix} 2 & 0 & 0 \\ 0 & 1 & 0 \\ 0 & 0 & 0 \end{vmatrix} \quad . \tag{5}$$

The vector polarization is +2/3, since 2/3 of the particles are in the substate $m_I = +1$, while there are none in the substate $m_I = -1$. The value 2/3 is actually the largest possible for pure vector polarization, since the density matrix must be positive definite with trace equal to unity.

The second set of equations (4) combine vector and tensor polarization of opposite signs; they do not correspond to pure tensor polarization. It can easily be shown, however, that the effects due to the tensor part alone can be obtained accurately by combining several measurements with different signs for the polarization of the incident beam.

In order to describe the scattering of polarized incident deuterons, it is convenient to introduce a different axis of quantization. Following

Raynal,[13] we take as z axis the direction of the incident deuteron on a target. The cross section for elastic scattering can then be written:

$$\frac{d\sigma}{d\Omega}(\theta,\phi) = \frac{d\sigma}{d\Omega}(\theta)\Big|_{n.p.} \Big[1 + t_{20}\rho'_{20} - 2\cos\phi\,(t_{11}\rho'_{11}+t_{21}\rho'_{21}) + 2\cos 2\phi\,(t_{22}\rho'_{22})\Big] \quad , \qquad (6)$$

where $\frac{d\sigma}{d\Omega}(\theta)\Big|_{n.p.}$ is the cross section with an unpolarized beam, the $\rho'_{\lambda,\mu}$ are the elements of the density matrix in the new frame of reference, and the $t_{\lambda\mu}$ are the polarization parameters describing the scattering. By taking measurements at different angles ϕ, it is possible in general to measure the various quantities $t_{\lambda\mu}$.

With a cyclotron, however, there is a limitation on the values of the $\rho'_{\lambda,\mu}$ which in practice excludes the possibility of measuring t_{21}. When the z axis is chosen parallel to the magnetic field at the ionizer, the density matrix simply reflects the occupation probability of the three magnetic substates; if the cyclotron magnetic field has the same orientation, this matrix will not be affected by the acceleration. If the orientation of the two fields were different, spin precession around the cyclotron magnetic field would take place in an uncontrollable fashion, since the length of time spent by all particles in the field is not the same. Thus, if the external beam is kept in the median plane of the cyclotron, the values of $\rho'_{\lambda,\mu}$ are limited, in effect, to the following:

$$\rho'_{1,1} = -\frac{i\alpha}{\sqrt{2}}\,,\ \rho'_{2,0} = -\frac{1}{2}\beta,\ \rho'_{2,1} = 0,\ \text{and}\ \rho'_{2,2} = -\frac{\sqrt{6}}{4}\beta \quad , \qquad (7)$$

where $\alpha = \rho_{1,0}$ and $\beta = \rho_{2,0}$. The cross section (Eq. (7)) becomes:

$$\frac{d\sigma}{d\Omega}(\theta,\phi) = \frac{d\sigma}{d\Omega}(\theta)\Big|_{n.p.} \left| 1 - \frac{\beta}{2} t_{20}(\theta) + i\alpha\sqrt{2}\, t_{1,1}(\theta) \cos\phi \right.$$

$$\left. -\sqrt{\frac{3}{2}}\, \beta\, t_{2,2}(\theta) \cos 2\phi \right| \quad . \tag{8}$$

Thus the tensor parameters t_{20} and t_{22} can be measured, but not t_{21}. This limitation does not exist when other accelerators are used; it is also possible, but usually inconvenient, to avoid this drawback even with a cyclotron by deflecting the external beam away from the plane perpendicular to the magnetic field of the cyclotron. However, as will be noted later, the ignorance of t_{21} is not usually a problem.

The method used to achieve the different states of polarization of the deuterons is in principle the same as for protons. However the Rabi diagram, shown in Fig. 2, is somewhat more complicated, and the possible transitions more numerous. To achieve pure vector polarization, for example, a low-field, a high-field, and a low-field transition are performed, in that order. The high-field transition exchanges the populations of states 2 and 5; the low-field transitions each can produce the following exchanges: 1-4, 2-3, and 5-6. If the second low-field transition is turned on and off during equal times, vector polarizations of +2/3 and -2/3 are obtained successively.

At ionization, two of the factors reducing the polarization values of protons are negligible for deuterons, viz, the background of H_2O and the magnetic field effect. Values very close to the theoretical maxima should thus be obtained.

Absolute Values of the Polarization

A) Protons.

It is important to have several well-established values of the absolute value of the polarization. Two such reference values are available, each with a precision of about 2%. The first is the polarization in the elastic scattering of protons from He^4; it has been measured by Rosen and Brolley[15] at 10 MeV. The second is the polarization in the elastic scattering of protons[16] from C at 45° (lab) and 15.7 MeV.

B) Deuterons.

Absolute reference values are not available. If the efficiencies of all the high-frequency transitions are measured, the polarization values should be close to the computed ones, except for background. But the background is essentially unmeasureable, so the polarization can be estimated with only limited accuracy. Further measurements are then necessary to obtain a precision of, say, 1%.

To calibrate the vector polarization, double scattering is a possibility. The tensor parameters t_{20} and t_{22} which enter the second scattering can be measured in a separate experiment with a tensor polarized beam with an error of several percent. Unless a tandem is used, t_{21} is more difficult to obtain. However, it is expected to be very small and can thus be evaluated sufficiently accurately from an optical model analysis which agrees with the other measured parameters. A heavy nucleus should be used as a target to avoid compound nucleus contributions and center-of-mass correction factors. Nevertheless, helium can also be a good target. The first scattering is then alpha particles on deuterium; the second is the scattering of the recoil deuterons from

He^4 at the same CM angle and energy. The tensor parameters t_{20} and t_{22} are again measured, but t_{21} is estimated from a phase shift analysis. The influence of uncertainties in the tensor parameters would be negligible.[17]

As soon as a calibration of the vector polarization is available, the other cases can be evaluated from the known efficiencies of the high frequency transitions.

Depolarization Effects in Accelerators

A) Tandems.

Depolarization can occur in the electron adding or stripping process for various reasons.[18] However it can usually be avoided by controlling the direction of spin precession with a magnetic field or by decoupling the nucleon spin from the electron spin with a high magnetic field.[19] Depolarization in the stripping process can also be minimized if the time allowed for charge exchange is very small, as it is, e.g., when thin foils are used.

B) Cyclotrons.

Depolarization can occur in cyclotrons during acceleration.[20] This can be best understood in a reference frame rotating at the mean Larmor precession frequency of the particle, ω_p. In such a frame, the effective magnetic field consists only in the small variations of the magnetic field. If these variations have an appreciable constant horizontal component in the rotating frame, depolarization may occur. (We assume that the main cyclotron magnetic field is vertical.) The condition that such a field exist is:

$$\frac{\omega_p}{\omega_c} = k + \ell\nu_2 + m\nu_x \quad , \tag{9}$$

where ω_c is the cyclotron frequency, $\nu_z\omega_c$ and $\nu_x\omega_c$ are the axial and radial betatron frequencies, and k, ℓ, and m are integers. This relation is a resonance condition. To compute the corresponding depolarization effects, the amplitudes of the betatron oscillations must be known, as well as the shape of the cyclotron magnetic field. Although calculations must be made for each individual case, it is usually found that depolarization is negligible, since it is very unlikely that the conditions for a resonance be satisfied for a large percentage of the ion acceleration time. Experiments have confirmed these predictions.

Polarized Beams by Other Methods

A) Metastable Hydrogen Atoms.

The Zavoiskii-Lamb[21] method uses a beam of hydrogen atoms in the $2S_{1/2}$ metastable state ($\tau_{1/2} \sim 0.1$ sec). The corresponding hyperfine structure is similar to the hyperfine structure of the ground state, as shown in Fig. 3. However, since the two lower $2S_{1/2}$ substates cross the two upper $2P_{1/2}$ substates, strong magnetic gradients are not needed to isolate the two upper $2S_{1/2}$ substates. Instead, at a field strength of 570 G, a small electric perturbation mixes the undesired substates with the very short-lived $2P_{1/2}$ substates ($\tau_{1/2} \sim 1.6 \times 10^{-9}$ sec). These quickly decay, so that the beam then contains ground-state and $2S_{1/2}$ upper substates in about equal proportions. The process is interesting if it is possible to produce an intense beam of $2S_{1/2}$ atoms and to ionize these selectively.

Two recent experiments make this method quite attractive. The first[22] showed that an intense beam of metastable hydrogen atoms could be produced by charge exchange in cesium vapor ($H^+ + Cs \rightarrow H_{2S_{1/2}} + Cs^+$). The second[23]

indicated that an electron could be added selectively to the metastable atoms by passing the beam through argon. The method is thus well-suited for tandems, and is being used at Wisconsin, Milan, and Los Alamos.

However, recent proposals[24] indicate that electrons can be added to the polarized atoms of a conventional source with high efficiency by charge exchange with negative hydrogen beams or cesium ions. Intensities in the microamp range should thus be produced; this is considerably beyond the probable current obtainable with the Zavoiskii-Lamb scheme. This charge exchange process should also be useful in obtaining positive ions from a standard source.

B) Polarized He^3.

Optically pumped polarized targets of He^3 are well known.[25] It has been suggested[25] that polarized beams of He^3 ions can be extracted from the He^3 cells, but no detailed values of intensity or polarization are yet available.

II. ELASTIC SCATTERING

A) Polarization and Asymmetry

Polarization parameters for the elastic scattering of protons were measured in double scattering experiments long before polarized ion sources were available. The standard experiment consists in scattering an initially unpolarized beam from the target of interest, and then analyzing the polarization of the scattered particles as a function of the angle θ between the direction of the scattering and the beam direction. To measure their polarization, these particles are scattered again from a convenient target whose

polarization properties are known, and the left-right asymmetry in the scattering is observed. The quantity measured is the polarization, $P(\theta)$:

$$P(\theta) = \frac{1}{P_p(\theta_p)} \frac{N_L - N_R}{N_L + N_R} \quad , \tag{10}$$

where N_L and N_R are the number of particles scattered to the left and right respectively after the second scattering, and $P_p(\theta_p)$ is the analyzing power of the second target at the angle θ_p of the second scattering. In terms of cross sections,

$$P(\theta) = \sigma_{++} + \sigma_{-+} - \sigma_{+-} - \sigma_{--} / \sigma_{++} + \sigma_{+-} + \sigma_{-+} + \sigma_{--} \tag{11}$$

Here, $\sigma_{++}(\theta)$ is the cross section for scattering from the first target with initial and final spins up, σ_{+-} is the cross section for scattering from an initial spin-up state to a final spin-down state, etc.

Double-scattering experiments can also be performed by exchanging the two targets of the previous type experiment. They correspond then with experiments done with beams from polarized ion sources since the beam incident on the target of interest is polarized. The measured parameter is now the asymmetry $A(\theta)$ in the scattering cross sections for spin-up and spin-down particles. It can be measured by counting the number of particles scattered at equal angles on the left and right sides of the beam. If the sign of the polarization of the beam is reversible, the same quantity is measured by counting the particles

scattered to one side only during equal times of spin-up and spin-down incident beam. The two quantities are the same because the axis of quantization, $\hat{n}$, effectively flips the spin of the incoming proton in scattering to the left and right:

$$\hat{n} = \hat{k}_i \times \hat{k}_f \quad , \tag{12}$$

where $\hat{k}_i$ and $\hat{k}_f$ are unit vectors specifying initial and final center-of-mass momenta. The asymmetry is thus:

$$A(\theta) = \sigma_{++} + \sigma_{+-} - \sigma_{-+} - \sigma_{--}/\sigma_{++} + \sigma_{+-} + \sigma_{-+} + \sigma_{--} \tag{13}$$

When spin flip is forbidden, as in elastic scattering on a target whose spin is not zero, $A(\theta)$ is equal to $P(\theta)$. In other processes, however, σ_{+-} and σ_{-+} are not generally zero, nor are they necessarily equal. Thus, in inelastic scattering, e.g., the measured asymmetry and polarization may be different. When it does not cause confusion, however, "asymmetry" and "polorization" will be used interchangeably.

B) Protons

Much of the data on polarization in the elastic scattering of protons are summarized in Ref. 26; the results which have appeared since the Karlsruhe Conference are noted in Table I.[27-41] The optical model parameters of Table I are defined by the following equation:

$$U(r) = V_c(r) - Vf(x_o) - i(W-4W_D d/dx_I)f(x_I) + (\hbar/m_\pi c)^2(V_s + iW_s)\underset{\sim}{\sigma}\cdot\underset{\sim}{\ell}(1/r)(d/dr)f(x_{so}) \quad , \tag{14}$$

where the Woods-Saxon form factors are given by:

$$f(x_k) = (1 + \exp(x_k))^{-1}$$

and

$$x_k = (r - r_k A^{1/3})/a_k \quad .$$

The first term is the Coulomb potential of a proton in the field of a uniformly charged sphere.

Although the data range over almost the entire periodic table, there are still large gaps, particularly for heavy nuclei. Detailed studies of nucleus to nucleus variations are available generally only at energies below 20 MeV. Boschitz[42] has found large anomalies in the 18.5 MeV elastic polarization around A=40, and smaller effects at A=90 and 208. His optical model analysis traces these to a decrease in the effective strength of the spin-orbit potential near the "closed" shells. The variations in the measured polarizations noted earlier by Rosen[26] occurred only at back angles and only at energies and mass numbers such that the nuclear size just permitted an integral number of wave lengths of the incident proton to fit into the potential. They have been well explained by optical model analyses. In other studies in which several neighboring nuclei have been measured, best-fit optical-model analyses[29,38] have yielded parameters of the spin-orbit potential which fluctuate from nucleus to nucleus. The amount of data available to study such variations is still small, so that a qualitative interpretation in terms of nuclear structure remains an interesting task.

1. Optical Parameters

Optical model analyses of cross-section and polarization data at approximately the same energy have now been carried out successfully at energies up to 50 MeV (see Table I). Only in rare cases,[28,32,35] in particular for C^{12} and Ca^{40}, has it been difficult to obtain good fits to both simultaneously. Such a procedure always involves some change in the parameters that are obtained by fitting either the cross section or the polarization individually, but the best-fit χ^2 normally is not much affected.

In order to detect systematic variations over the range of nuclei examined, most authors have tried to find an average set of parameters. The values of χ^2 obtained with the average set are usually two to three times worse than those obtained with best-fit parameters. However, no one has yet attempted to find a set of geometrical parameters that is equally good at all energies between 10 and 50 MeV. This of course would be an enormous task, complicated by the relative lack of data at the high energy end of the range; it is also not evident a priori that such a set exists. It is interesting to note, however, that the parameters obtained by Satchler[35] at 30 MeV have been tried successfully at 18.6 MeV,[30] with the spin-orbit radius reduced by about 10%. The average parameter set found by Fricke et al.[38] at 40 MeV also resembles that of Satchler, at least with respect to the relative values of r_I and r_0.

2. The Spin-Orbit Potential

Polarization data are generally expected to yield significant information about the shape and magnitude of the spin-orbit term in the optical potential. Since the magnitude of the polarization is proportional in first order to the

strength of the spin-orbit term,[43] V_s has indeed been fixed reasonably well at an average value between 5 and 7 MeV.

As accurate data have become available, it has also been possible to learn something about the shape of the potential. It is no longer supposed to be strictly of the Thomas type,[44] since the spin-orbit radius is now established to be about 10% smaller than the radius of the real central term.[28,43,45,46]

The Thomas shape was not firmly established since the origin of the $\underset{\sim}{\ell}\cdot\underset{\sim}{s}$ term is not definitely known. It had been suggested by its analog in atoms[47] although the Coulomb interaction is not nearly sufficient to account for the magnitude of the spin-orbit potential in the nuclear problem. More definite evidence[48] came from early attempts to derive the optical potential directly from two-nucleon scattering using the impulse approximation, a procedure which is justified at large proton energies. The spin-orbit potential was shown to have the form:

$$U_{so} = \left(\frac{\hbar}{m_\pi c}\right)^2 (V_s + iW_s)\underset{\sim}{\sigma}\cdot\left[\underset{\sim}{\nabla}(\rho(r))\times\frac{1}{i}\underset{\sim}{\nabla}\right] \quad , \tag{15}$$

where $\rho(r)$ is the nuclear matter density. Similar expressions[49] were also obtained by other authors using various approximations; they indicate that U_{so} arises chiefly from the nucleon-nucleon spin-orbit force. When $\rho(r)$ is spherically symmetric, the form becomes more familiar:

$$U_{so} = \left(\frac{\hbar}{m_\pi c}\right)^2 (V_s + iW_s)\underset{\sim}{\sigma}\cdot\underset{\sim}{\ell}\,(1/r)(d/dr)\rho(r) \quad . \tag{16}$$

Since the central potential is derived from the long-range part of the nucleon-nucleon force, and should thus extend beyond the nuclear density, it has been recently proposed by several authors[46,50] that the difference in radius parameters between the central and spin-orbit terms is quite natural. On the other hand, Satchler[35] has suggested that the difference in range between the forces should be reflected in different diffuseness parameters for the real central and the spin-orbit terms rather than different radii. Sprung and Bhargava[51] have suggested an alternative explanation based on nuclear matter calculations.

Shapes other than the modified Thomas form have been tried, but there is no evidence that they give better results. Hooper[52] has investigated a volume spin-orbit term in an effort to fit the 9.4 MeV data previously analyzed by Greenlees et al.[53] When r_{so} and a_{so} were kept at the corresponding values for the real central potential, the fits obtained were on the whole better than those obtained using a derivative type spin-orbit form factor with the same restrictions. When r_{so} and a_{so} were allowed to vary, not only did the derivative type form factor give the best overall fit for the polarization of Co, Ni[58], Ni[60], and Cu, but also the optimum r_{so} values showed much greater consistency among themselves. Kossanyi-Demay et al.[30] allowed the multiplicative factor in the modified Thomas form to take on values between $1/r^0$ and $1/r^2$, and then searched for U_o, W_d, U_{so}, and r_{so}. These modifications changed significantly only the final value of U_{so} and improved neither elastic nor inelastic fits.

Such calculations indicate that it is unlikely that more precise measurements of the polarization, except perhaps at the very forward angles,[43]

will define the shape of the spin-orbit term more precisely. At large angles the differential polarization is as sensitive to the central-well parameters as it is to the form of the spin-orbit term. However, it is possible that measurements of the parameters[13] R, D, and A will indicate the need for a different shape of potential. Such measurements are well within the capabilities of present polarized beams, and could be useful also in determining spin-spin forces in the optical potential, e.g.

Polarization Measurements Near Analog Resonances

Measurements of the polarization in elastic scattering near analog states have become extremely useful in the determination of the spin of resonances. The assignment is more definite than the one which can be made for the parent state by the observation of J dependence in one-nucleon transfer cross sections, and the method is best applied in the heavier nuclei where the latter does not appear useful. It is also simply explained.[54] The polarization occurs because of the interference between the compound nucleus and optical model amplitudes at the resonance, and can be fitted very nicely by adding the appropriate Breit-Wigner resonance terms to the optical model amplitudes. To determine spins, the calculations of Adams et al.[54] show that in principle it is often necessary to take data at only one angle and energy, though in practice a few extra data points add assurance and a detailed study can determine with precision other resonance parameters as well.

The number of spins assigned in this way is small, but bound to increase rapidly as more tandems begin operation with polarized sources. The method was first applied by Moore and Terrell[55] to the study of a previously measured resonance in $Zr^{90}(p,p)$ at 6.71 MeV. Figure 4 shows the impressive data obtained

with the Wisconsin polarized beam for elastic scattering on Ce^{140} between 9 and 12 MeV.[56] Five resonances occur in this region, the third of which corresponds to a state which had been previously assigned 3/2-. The fit obtained shows that this state is clearly 1/2-. The good fit is interesting because the resonance energies are close to the Coulomb barrier so that the optical parameters begin to be important and also because several resonance terms with the same ℓ had to be added to the optical potential.

C) Deuterons

The polarization in the elastic scattering of deuterons is in principle considerably more complicated than that of protons, as indicated in the discussion of Section I. The description of deuteron scattering via the optical model is also more complicated than for protons. In addition to the real and imaginary central terms, and an $\underset{\sim}{L} \cdot \underset{\sim}{S}$ term, three kinds of tensor potentials are now allowed by general arguments.[57] One of the three types can arise both from the D state admixture to the deuteron wave function and from nucleon-nucleus $\underset{\sim}{L} \cdot \underset{\sim}{S}$ potentials. Calculations indicate that these two sources give non-zero contributions and do not cancel each other.[13,58] The other two types have not been calculated.

Vector and tensor parameters have been measured for Ca^{40}, Ni^{60}, Zr^{90}, and Pb^{208} at 22 MeV;[59,60] some of these are illustrated in Figs. 5 and 6. The two types of data are now also available for Al^{27}, Si^{28}, and Ni^{60} between 7 and 11 MeV.[61] The vector polarization of 22 MeV deuterons scattered from C^{12}, Si^{28}, and Ni^{58} is also known.[62] A complete analysis of the Ca^{40} cross-section and polarization data has been made by Raynal;[63] preliminary analyses of the low energy results have also been made.[61] Raynal found best agreement

with the Ca^{40} results by setting the tensor potentials to zero; this result is surprising in view of the above-mentioned predictions. The analysis of the light-element data by Schwandt gives evidence that tensor potentials with a strength of about 2 MeV are necessary, but the fits at this stage are not very satisfactory. All optical model analyses indicate that t_{21} is very small.

The $\underset{\sim}{L} \cdot \underset{\sim}{S}$ potential determined for Ca^{40} had a strength of 6.5 MeV; a similar value is indicated by the low energy analysis. It is interesting to note also that the spin-orbit radius Raynal found was smaller than the radii of the central terms; a similar result was later obtained for proton elastic scattering as mentioned above. There is evidence from Schwandt's analysis that this remains valid at lower deuteron energies as well.

Diffraction models[64] have also been used to interpret the elastic polarization of deuterons (and other particles). All partial waves which, classically, strike the nucleus are assumed completely absorbed, and the real part of the scattering amplitude is neglected. Surprisingly good fits have been obtained when the experimental cross sections are used in computing the polarization. In order to obtain detailed knowledge of the tensor and spin-orbit potentials, however, many more optical-model analyses must be performed; some data for them already exist, but much more are necessary.

D) He^3 and H^3

The spin-orbit term in the optical potential for He^3 and triton-nucleus scattering is still essentially unknown. It has a negligible effect on the differential cross sections, and all analyses[65] have been made without

it. Burcham et al.[66] have measured the polarization of initially unpolarized 29-MeV He^3 ions elastically scattered from C, Sn, and Au. These data, together with strong-absorption model fits by Frahn and Wiechers,[67] are shown in Fig. 7. Since most of the data points are consistent with zero polarization, the assigned spin-orbit strengths of 7 MeV for C^{12} and 6 MeV for Sn are quite tentative. It is interesting, however, that the polarization at angles larger than 60° is predicted to be quite large. Beery et al.[68] have looked at the double scattering of 21 MeV tritons from both Ni and C at primary angles as large as 31° and secondary angles up to 60°; they saw no polarization within their errors. At angles larger than these, the counting rate was too small to obtain useful statistics.

III. INELASTIC PROTON SCATTERING

There are now the beginnings of a systematics on asymmetries in the inelastic scattering of polarized protons. The incident energies range from 16.5 to 50 MeV, the targets are as heavy as Mo^{92}. The choice of experiments has thus far been imposed mostly by such factors as the energy and quality of available polarized beams and the resolution of the detectors. These limitations are changing rapidly, and many different types of states can be studied in the near future.

Table II[41,69-75] lists the available results. Our discussion of them will be ordered by the theoretical interpretations presently possible. The distorted-wave Born-approximation (DWBA) or the coupled-channels method are necessarily used; both demand the evaluation of radial matrix elements or form factors. This can be done most simply via the macroscopic model

which will be reviewed first, in connection with the collective levels it was designed to describe. Attempts to fit the data for Fe^{54} with a phenomenological microscopic model will be discussed next. This will lead to consideration of a realistic microscopic model which opens up the possibility of obtaining information on nuclear structure or the effective nucleon-nucleon force directly from differential polarization data. We will indicate the limitations of present microscopic calculations, and consider the effects of antisymmetrization. Finally, the possibilities for measuring the spin-flip interaction strength will be briefly mentioned.

Macroscopic Model and Collective States

A) Rotational Nuclei

The best region in which to study polarization for collective states is the rare earths; the very successful coupled-channels analysis of inelastic alpha scattering[76] on these nuclides indicates the possibilities. For experimental reasons the only polarization data available for rotational nuclei, however, concern the magnesium isotopes, Mg^{24}, Mg^{25}, and Mg^{26}. Preliminary asymmetry distributions[71] for ℓ=2 transitions at 20 MeV are illustrated in Fig. 8; several ℓ=2 curves for Al^{27} and Si^{28} whose deformations are not known are also shown. Data were taken every five degrees; the errors are generally $\pm$ 0.03. Since few attempts at fitting these data have yet been made, it is not yet known whether the variations in shape from one curve to the next can be accounted for in terms of the simple rotational model. Results for 0^+ and 3^+ states have also been obtained.

B) Vibrational Nuclei

The usual starting point for the vibrational model is to assume that the

nuclear surface should be represented by the following shape,

$$R(\theta,\phi) = R_o(1 + \Phi(\theta,\phi)) \quad , \tag{17}$$

where $\Phi(\theta,\phi) = \sum_{\lambda\mu} \alpha^*_{\lambda\mu} Y^*_{\lambda\mu}(\theta,\phi)$, and the $Y_{\lambda\mu}(\theta,\phi)$ are the usual spherical harmonics. Two methods[77] have commonly been used to represent the effect of such deformations on the optical potential U(r) of Eq. (14). The first is to replace U(r) by $U(r-R_o\Phi)$. The surfaces $(r = r_o + R_o\Phi)$ are then equipotential surfaces; one of these is given by $(r = R(\theta,\phi))$. The other standard method is to replace R_o, wherever it occurs in the undeformed potential, by $R(\theta,\phi)$. If r always appears in the combination $(r-R_o)$ this method is equivalent to the above one. If r does not occur in this form, as in the spin-orbit potential defined by Eq. (16), the two methods diverge and equipotential surfaces cannot be easily defined. In particular $(r = R(\theta,\phi))$ is not an equipotential surface.

Hill[77] has suggested that a more consistent transformation of the optical potential would consist in replacing U(r) by $U(r/1 + \Phi(\theta,\phi))$. The equipotentials are then surfaces of constant density, $(r = r_o(1 + \Phi(\theta,\phi))$; two of these are given by $(r = R(\theta,\phi))$ and $(r = 0)$. The potential is then unique at $(r = 0)$, a condition that is satisfied by neither of the potentials defined above.

The DWBA expression[78] for the differential cross section for unpolarized projectiles and unpolarized target nuclei is

$$\frac{d\sigma}{d\Omega} = \frac{\mu_a\mu_b}{(2\pi\hbar^2)^2}\frac{k_b}{k_a}\quad\frac{\Sigma|T|^2}{(2J_A + 1)(2s_a + 1)} \quad , \tag{18}$$

where μ_a and μ_b are the reduced masses of the incoming and outgoing particles, k_a and k_b are their wave numbers, J_A is the spin of the target nucleus and s_a is the spin of the incident particle. The sum is over the magnetic quantum numbers M_A, m_a, M_B, and m_b. The transition amplitude T can be written:

$$T_{DW} = J\int d\underset{\sim}{r}_a \int d\underset{\sim}{r}_b \; X_b^{(-)*}(\underset{\sim}{k}_b, \underset{\sim}{r}_b) \langle B,b|V_{eff}|A,a\rangle \; X_a^{(+)}(\underset{\sim}{k}_a, \underset{\sim}{r}_a) \quad . \tag{19}$$

Here $\underset{\sim}{r}_a$ is the displacement of the incoming particle a from the target A, $\underset{\sim}{r}_b$ the displacement of the outgoing particle b from B, and J is the Jacobian of the transformation to these relative coordinates. The functions $X_b^{(-)}$ and $X_a^{(+)}$ are the distorted waves which describe the elastic scattering of the incident and outgoing particles. In inelastic scattering, when exchange is neglected and V_{eff} is assumed local, $\underset{\sim}{r}_a$ and $\underset{\sim}{r}_b$ are equal and J is unity.

In the vibrational model, B is represented by a phonon creation operator acting on the zero-phonon ground state A; the effective interaction is the first order term in a Taylor expansion of the deformed optical potential $U(r,\theta,\phi)$. The radial shape of the matrix element or form factor $\langle B,b|V_{eff}|A,a\rangle$ and thus the shape of the angular distribution depend on the form of V_{eff}. The central terms, real and imaginary, in the effective interaction are the same in method (1) above as in method (2), since r appears only in the form $(r - R_o)$:

$$V_{cen}^{(1)}(r) = V \frac{R_o}{a}(1+e)^{-2} e + iW \frac{R_o}{a}(1+e)^{-2} e + i4W_D \frac{R_o}{a} e(e-1)(1+e)^{-3} \quad , \tag{20}$$

where $e = \exp(r - R_o/a)$. In method (3), the factor R_o is replaced by r. The spin-orbit part of the effective interaction in the three methods is as follows:

$$1)\quad V_{so}^{(1)}(r) = \left(\frac{\hbar}{m_\pi c}\right)^2 V_{so}\,\frac{R_o}{a^2 r^2}\;2e(1+e)^{-3}\,\{a(1+e) + r(e-1)\}$$

$$2)\quad V_{so}^{(1)}(r) = \left(\frac{\hbar}{m_\pi c}\right)^2 V_{so}\,\frac{R_o}{a^2 r^2}\;2e(1+e)^{-3}\,\{r(e-1)\} \qquad (21)$$

$$3)\quad V_{so}^{(1)}(r) = \left(\frac{\hbar}{m_\pi c}\right)^2 V_{so}\,\frac{1}{a^2 r}\;2e(1+e)^{-3}\,\{a(1+e) + r(e-1)\}$$

The expressions (21) all assume a spin-orbit potential of the form given by Eq. (16); the non-radial terms of Eq. (15) are neglected. When the latter are included,[79] and the nuclear density is written as follows,

$$\rho(r) \sim \rho(r,R_o) + \frac{\partial\rho}{\partial R_o}(r,R_o)\Phi(\theta,\phi)\quad , \qquad (22)$$

the deformed spin-orbit potential can then be written:

$$V_{so}(r,\theta,\phi) = \left(\frac{\hbar}{m_\pi c}\right)^2 (V_s + iW_s)\underset{\sim}{\sigma}\cdot\left[\underset{\sim}{\nabla}\,\frac{\partial\rho}{\partial R_o}\,\Phi(\theta,\phi) \times \frac{1}{i}\,\underset{\sim}{\nabla}\right] . \qquad (23)$$

This can be decomposed into a radial term $V_{so}^{(1)}(r)$ which corresponds to method (2) above, and an angular-dependent term $V_{so}^{(2)}(r,\theta,\phi)$:

$$V_{so}^{(2)}(r,\theta,\phi) = \left(\frac{\hbar}{m_\pi c}\right)^2 (V_s + iW_s) \frac{\partial \rho}{\partial R_o} \underset{\sim}{\sigma} \cdot [\underset{\sim}{\nabla}\Phi(\theta,\phi) \times \frac{1}{i} \underset{\sim}{\nabla}] \qquad (24)$$

Since the origin of the spin-orbit term in the optical potential is not well-known, the choice among these expressions for the deformed spin-orbit potential is not determined a priori, and can only be justified by experiments.

1. ℓ=2 Transitions

Strong ℓ=2 transitions in Fe^{56} and the Ni isotopes have been analyzed with the vibrational model; the experimental curves agree quite well with the predictions at both 18.6 MeV and 40 MeV,[75] except at angles smaller than 50°. The interpretation of the Oak Ridge 40 MeV results showed the importance of including the distortion of the imaginary and the spin-orbit potentials in a full collective-model analysis. Because the strength of the spin-orbit term is so much smaller than that of the central terms, the effects of its vibrations have gone unnoticed in the measurements of differential cross sections alone. However, the polarization at 40 MeV is very sensitive to the $\underset{\sim}{\ell} \cdot \underset{\sim}{\sigma}$ term in the interaction, and a good fit to the data with the DWBA could not be achieved without it. Figure 9 illustrates the effect of various interaction terms on the predicted cross section and asymmetry for Ni^{60} at 40 MeV. Similar fits, very good at angles larger than 50°, were also obtained for 2^+ excitations in Si^{28}, Fe^{54}, and Ni^{58}.

The distorted spin-orbit term is less important[70] at 18.6 than at 40 MeV, as shown in Fig. 9. While it always improves the fits to collective states at least slightly, its effect is large only when it is assumed to

have an unreasonably large magnitude. Nevertheless, the predicted curve agrees reasonably well with the data; somewhat better fits were obtained for ℓ=2 transitions in the Ni isotopes and Cu^{63}.

Method (2) was used for the 40-MeV calculations while method (1) was used at 18.6 MeV. The predicted polarizations using the two methods at the same energy show neglegible differences. On the other hand, Blair and Sherif[79] have recently shown that the distortion of the non-radial terms in the spin-orbit potential can improve the collective model fits at 40 MeV. This is the first evidence that such terms should be included in the optical potential. Further evidence could also arise from the analysis of differences in the polarization in elastic scattering on neighboring deformed nuclei, the one with spin and the other with spin zero. The limited data of this type have been analyzed thus far only with a spherically symmetric form for the spin-orbit potential.

2. ℓ=3 Transitions

Precise asymmetry data on octupole transitions in Ca^{40}, Zr^{90}, Zr^{92}, and Mo^{92} at 20 MeV are now available;[71] the ℓ=3 data in the Ni region are less abundant than the ℓ=2 data there and the statistics are poorer. Only the distributions in the Ni region have yet been analyzed; the collective model shows fair agreement. The 40 MeV predictions are again more sensitive to the distorted spin-orbit term, but the analyzed data are not sufficient to determine whether it is necessary.

3. ℓ=4 Transitions

Good differential asymmetries have been measured for ℓ=4 transfer in the light rotational nuclei at 20 MeV;[71] these demand a coupled-channels

analysis which has not yet been carried out. Supposed $\ell=4$ transitions in Fe^{54} and Ni^{58} have also been studied at 18.6 MeV;[70] the experimental asymmetry distributions are quite different and neither is fit well with the coupled-channels code assuming reasonable collective model parameters and direct or two-step excitation via the first 2^+ state only.

4. Fe^{54}

The asymmetry measured for the $\ell=2$ transition to the 1.41-MeV first excited state in Fe^{54} at a proton energy of 18.6 MeV presents a special problem in interpretation.[70] The data, shown in the upper half of Fig. 10, reveal much larger asymmetries at 30° and 90° than those obtained for the neighboring 2^+ vibrational levels discussed above. The asymmetries for the second 2^+ state resemble the Fe^{56} data. (The theoretical curves are discussed below.) Data for Cr^{52} and Ti^{50} are, on the other hand, quite similar to the Fe^{54} 1.41-MeV results. These variations between the shapes measured for the first 2^+ states of N=28 nuclei and their more collective neighbors are too large to be explained by the vibrational model. Corresponding variations in the shape of differential cross sections[80] have also been observed.

Microscopic Model

Such data indicate the need for a microscopic description of the reaction which takes into account the detailed structure of the initial and final states. Calculations of this type have been performed in recent years by several authors.[81,82,83] The nuclear states are treated as accurately as possible, and the interaction between the incoming nucleon and the nucleons of the target is assumed to be closely related to the free nucleon-nucleon

interaction. Depending on the configurations necessary to describe the states involved, the form factors can thus assume many different shapes, whereas in the vibrational model the form factor has the same shape for all one-phonon states in the same nucleus.

The asymmetries for the first two 2^+ states in Fe^{54} have been compared with the predictions of the microscopic model by Satchler.[83] The ground state was assumed to be an $(f_{7/2}^{-2})^{0^+}$ proton configuration, and the 1.41- and 2.97-MeV states were taken as $(f_{7/2}^{-2})^{2^+}$ and $(f_{7/2}^{-3}p_{3/2})^{2^+}$ proton configurations respectively. A Yukawa interaction with a range of 1 F was assumed. The 18.6-MeV predictions, shown with the data in Fig. 10, do not agree well for either state; in fact, the fits resemble those obtained with the collective model with a real form factor only.

Phenomenological calculations have also been carried out[70] in which the parameters of the collective model form factor have been varied. Such variations have not produced a good fit to the Fe^{54} data, but they do modify and improve the agreement. More generally, they indicate that the predicted asymmetry is sensitive to the form factor, and thus that asymmetry measurements could lead to nuclear structure information. Calculations by Glendenning et al.[81,84] with realistic wave functions for the Ni isotopes also predict marked variations of the asymmetries as a function of the nuclear configurations.

The Nuclear Wave Functions

The best region in which to carry out tests of the microscopic model is near closed shells, where the wave functions can be calculated with some degree of assurance. Thus cross sections[83,84] for O^{18}, Ca^{40}, Ni, Zr, and Pb^{208} have been compared with the predictions of the model; the transitions

include both strongly collective and apparently simple excitations. Polarization data are now available at 20 MeV for Ca^{40}, Zr^{90}, Zr^{92}, and Mo^{92}, but these have not yet been analyzed.[71]

The necessity of using accurate wave functions has recently been emphasized by Love and Satchler.[85] They have shown that core polarization can account for as much as 80% of the cross section in such an apparently simple case as the excitation of the first 2+ state in Zr^{92}. They were able to evaluate the influence of the neglected configurations in a non-arbitrary way by calculating an effective charge from known electromagnetic transition rates. An additional, phenomenological form factor was thus added to the microscopic form factor for the computation of cross sections; it has just the same shape as the standard vibrational model form factor, including, in principle, imaginary and spin-orbit terms. The effect of this addition on predicted asymmetries has not yet been evaluated.

Such collective admixtures could be important even for the so-called single-particle transitions which would otherwise be ideal for study. It is interesting to note that even if the contributions of the core nucleons to these wave functions could be known exactly, there would still be a residual effect on the cross sections attributable to the "core polarization" of Love and Satchler. With a real effective interaction, these extra configurations would add only a real term to the form factor, whereas the "core polarization" form factor is complex, as mentioned above.

The Effective Force

If the nuclear wave functions are assumed to be exact, Glendenning[86] has shown that the off-diagonal matrix elements of the effective interaction can

be written:

$$\mathcal{V}_{\alpha\beta} = V_{\alpha\beta} + \sum_c \frac{\langle \phi_{\alpha J} | V | \psi_c \rangle \langle \psi_c | V | \phi_{\beta J} \rangle}{E - E_c + i\epsilon} \qquad (25)$$

Here V is the free nucleon-nucleon force, ϕ_α and ϕ_β are the initial and final states of the target nucleus, and the sum over c includes all the states of the target plus incoming nucleon system which are not explicitly included in the coupled-channels calculation. As it stands, $\mathcal{V}_{\alpha\beta}$ is complex, energy-dependent, and non-local, and impossible to evaluate exactly. However, the second term of Eq. (25) has always been neglected for reasons of simplicity; moreover it is a sum over many small terms which appear with fluctuating signs and thus is probably small. In actual calculations, the two-body potential V itself is also approximated to be of the following local form:

$$V_{ij}(r_{ij}) = (V_o + V_1 \, \underset{\sim}{\sigma}_i \cdot \underset{\sim}{\sigma}_j) g(r_{ij}) \quad . \qquad (26)$$

Each term gives rise to a form factor; the second term alone contributes to transitions with a spin transfer S=1. The radial shape of the potential, $g(r_{ij})$, has normally been assumed to be of either Guassian or Yukawa form. The parameters V_o and V_1 also depend on isotopic spin in the following way:

$$V_s = V_{s\alpha} + V_{s\beta} \, \underset{\sim}{\tau}_i \cdot \underset{\sim}{\tau}_j \quad , \qquad (27)$$

where s has the values 0 or 1.

A considerable effort is necessary to determine these parameters accurately at many energies. The evaluation of the range of the force demands knowledge of the different multipoles at each energy. Inelastic scattering experiments measure $V_{s\alpha} \pm V_{s\beta}$, depending on whether the excited nucleons of the target and the incident nucleons have the same τ_z (+ sign) or different τ_z (- sign). Since $V_{o\beta}$ is expected to be smaller than $V_{o\alpha}$, a more direct measure of $V_{o\beta}$ is the cross section in (p,n) or (He^3,t) reactions between analog states;[87] fits to cross sections[83] are, however, not very satisfactory thus far and polarization data exist only for very light nuclei.[88] Tensor and spin-orbit terms must a priori also be included in the two-body potential V_{ij}; their influence is not yet established.

Typical values for the parameters of V_{ij} obtained by Love and Satchler[85] with a Yukawa potential of range 1F are as follows:

$$V_{o\alpha} \sim 80 \text{ MeV}, \quad V_{o\beta} \sim 20 \text{ MeV}, \quad V_{1\alpha} \sim 40 \text{ MeV}, \quad V_{1\beta} \sim 10 \text{ MeV}.$$

These strengths were used in the analyses of inelastic scattering and (p,n) reactions on O^{18}, $Zr^{90,92}$, and Pb^{208} at around 20 MeV. Core polarization was included.

S=0 and S=1 Interactions

A clear experimental separation of the contributions from S=0 and S=1 interactions does not seem possible with asymmetry measurements. It is difficult, first of all, to find states for which only the S=1 interaction should be important and which might thus serve as a calibration of spin-flip polarization. Unnatural parity states (i.e., states for which the parity does

not equal $(-1)^J$, where J is the spin of the level) are one possibility, since they cannot be reached in first order by an S=0 interaction; however, higher order S=0 excitation could be important. When both S=0 and S=1 are allowed, the predicted asymmetries hardly distinguish between them provided the form factors are the same for each.[70,89] The predicted polarization of the outgoing particle after a $1f_{7/2}$ to $2p_{3/2}$ inelastic transition, for example, is approximately the same whether S is zero or one. On the other hand, when many configurations contribute to the excitation of a particular state, the form factors for S=0 and S=1 transfer are not necessarily similar, and in this case the predicted asymmetries do depend on the spin transfer.[84]

The interference between S=0 and S=1 contributions to the asymmetry has been small in calculations reported thus far.[70,89] As a consequence, the difference between the asymmetry and the corresponding polarization measured with an unpolarized incident beam is expected to be small. The magnitude of these differences has been proposed[90] as a measure of the S=1 interaction strength.

One possibility which remains is the measurement of the spin-flip cross section. However, there is still no direct relationship between the cross section and V_1, since the spin-orbit part of the optical potential contributes to the spin-flip cross section even for S=0. In fact, in the few analyses[91,92] reported to date, it has not been necessary to invoke S=1 transfer, although the distorted spin-orbit term is important.[92] Spin-flip cross sections have all been measured in $(p,p'\gamma)$ or $(n,n'\gamma)$ experiments; only transitions to 2+ states which have a gamma branch to the ground state have thus been observed. There would be no such spin limitation in the direct measurement of spin-flip

by analyzing the change in polarization in the inelastic scattering of an initially polarized beam.

Antisymmetrization

With the exception of some recent work of Amos, McCarthy, and Madsen,[93] almost all microscopic model calculations have been carried out by neglecting the effects of the antisymmetrization of the incoming nucleon with the target nucleons. When space exchange is included the form factor description is no longer valid and the computation becomes difficult. The studies of Amos et al.[93] and later computations by Madsen[94] show that such exchange contributions can be very important in their effect on the magnitudes and shapes of cross sections. In particular, the ratio of the cross section predicted at large angles to that predicted at the forward maximum is often considerably increased.

It is then interesting that the standard DWBA had difficulties in fitting the results for the 28-neutron nuclei where the excited states are presumed to be predominantly proton configurations, while the predominantly neutron configurations of the collective states agreed well with predictions. As well as giving poor fits to the polarization, the DWBA underestimated the back angle cross section of the proton states. A comparison of the preliminary experimental data for Zr^{92} and Mo^{92} reveals the same features.[71] At large angles the relative cross section for the 0.93 MeV 2^+ state in Zr^{92}, presumably made up chiefly from neutron excitations, is smaller than that for the 1.51-MeV 2^+ state in Mo^{92}. The measured asymmetries for Mo^{92} are also more positive than those measured for Zr^{92}. A most appealing explanation of the observed differences then might reside in space and spin exchange contributions, which can effect the distributions only for proton states, since charge exchange is small. Such a suggestion of course remains tentative until the effect of

antisymmetrization on the asymmetry has been calculated.

The comparison of proton and neutron inelastic scattering to the same states is also useful in this regard. A limited amount of data exist on the scattering of 14-MeV neutrons[95] from the first 2^+ states of Cr^{52} and Ni^{58}. Within rather large errors, the results for the two nuclei are similar, which is not the case with protons incident.

Antisymmetrization effects are also expected to be more important for higher multipoles but less important as the energy increases.[94]

IV. TRANSFER REACTIONS

Pickup and stripping reactions have been producing important spectroscopic information for years.[96] Their utility is based on the apparent simplicity in the interpretation of spectra and differential cross sections, especially if only one particle is transferred. The angular distributions determine the orbital angular momentum transferred and, very often, the total angular momentum transferred. Absolute spectroscopic factors have been extracted as well, using the distorted-wave method. However, the reliability of at least these absolute numbers depends on how accurately the DWBA describes the reaction. Since the polarization of the outgoing particles can be measured as well as their intensity, one should demand that the DWBA be able to predict the polarization also. Polarization measurements are then interesting from two points of view: They can provide information on the J transfer, as is well known, and they can also serve as a sensitive test of the DWBA and competing reaction models.

A) The Data

Not many results are available, however; these are reviewed in Table III.[97-128] Most of the experiments listed have been performed at energies where the direct reaction mechanism should predominate. Since the majority involve light nuclei as targets, however, compound nucleus contributions can be ruled out in just a few cases. In most of the work, the statistical errors are quite large. Only preliminary data are available on the (p,t) reaction at high energy; Chant[126] has looked at C^{12} and O^{16}(p,t) reactions at 30 MeV and found large polarizations. Measurements of tensor polarization parameters are also very scarce; only two sets are included in Table III, and both concern the very light nucleus Be^{9}. It is confidently expected that this situation will soon change.

1. ℓ=0 Transfer

It has often been emphasized[129,130] that ℓ=0 transitions are the simplest to analyze. In the semiclassical picture of Newns,[131] where no spin-orbit interaction was considered, the polarization in ℓ=0 transfer was exactly zero. Now it is clear that both proton and deuteron spin-orbit distortions must be included, but these can be reasonably treated in first-order except when the polarization is close to 100%.[130] In this way, Johnson[130] has derived a relationship between polarization and asymmetry measurements in (d,p) reactions which includes the effect of the D state of the deuteron:

$$P = P(p,SS) + P(d,SD)$$
$$A = \frac{2}{3} P(p,SS) + P(d,SD) + P(d,SD) \qquad (28)$$

Here, P is the proton polarization measured with an unpolarized deuteron beam, and A is proportional to the asymmetry in the proton distribution in a reaction initiated by vector polarized deuterons. The contributions from the S- and D- wave parts of the deuteron wave function are coherent; those from the proton and deuteron spin-orbit terms are additive. The notation implies, then, that P(p,SD), e.g., is the contribution to the polarization arising from the proton spin-orbit force, and that this is the interference term, the contribution linear in both S and D waves.

In a calculation which included only S waves in the deuteron wave function, Hooper[129] showed that the deuteron spin-orbit term should have little effect on ℓ=0 polarization, so that P(d,SD) is presumably small also. In that case, a measurement of P and A together determines directly the effect of the D state in the proton channel, P(p,SD). If P(d,SD) is large the determination of P and A together is still useful, since (P - A) is independent of P(d,SD). Some data do exist[102,121] which do not fulfill the simple relation, A=2/3 P, but the center of mass energies are not exactly the same and the statistics, especially for P, are not sufficient. These can be improved by measuring instead the asymmetry in the deuteron distribution in the inverse (p,d) reaction with polarized protons.

The fact that the deuteron spin-orbit potential is apparently unimportant for ℓ=0 transitions probably explains the relative success of the DWBA for such transitions, at least for polarization in light nuclei. Fits to Mg^{24}(d,p) and Si^{28}(d,p) polarization data[101] are shown in Fig. 11. It probably also accounts in part for the surprising success of the simple absorption model of Walls.[132] He assumed that only one proton partial wave is important (this

has some support from Hooper's analysis[129] of L-space localization), and that this partial wave is distorted by a spin-orbit potential only. His fits to ℓ=0 polarization are at least as good as those obtained with the DWBA.

2. $\ell > 0$ Transfer

No simple correlation between asymmetry and polarization can be predicted if ℓ is greater than zero. However, the measured differential polarizations themselves are interesting from the point of view of J dependence. Even the simplest reaction models predict that the polarization is sensitive to the total angular momentum transferred. But the data must be carefully examined for evidence that the differences are consistent over a reasonable range of nuclei and energies.

In the most extensive study of J dependence in heavier nuclei to date, Yule and Haeberli[119] found consistent results for Mg^{24}(d,p), Ca^{40}(d,p), and Cr^{52}(d,p) for ℓ=1, ℓ=2, and ℓ=3 transfers; measurements were taken with 7 and 8 MeV polarized deuterons. Four 3/2-, three 1/2-, two 3/2+, and one 5/2+, 5/2-, and 7/2- distribution were studied, generally over an angular range extending from about 15° to 65°, though the 5/2- measurement included only three angles. These data are shown in Fig. 12; they are reasonably well explained by the DWBA. If deuteron absorption is more important than proton absorption, semi-classical theories predict that $j=\ell+1/2$ polarizations are positive near the stripping peak, and $j=\ell-1/2$ distributions are negative. (This is true even when the effects of the spin-orbit potential are included in the semi-classical models, as discussed quite clearly by Butler in Ref. 133.) It is interesting to note that the ℓ=1 and ℓ=2 distributions agree with these expectations while the ℓ=3 asymmetries show the opposite behavior. Rollefson

et al.[127] have measured four ℓ=1 polarizations in Ni^{58}(d,p) at 15 MeV over the range of 10° - 30° which includes the stripping peak. The results are positive for 3/2-, and negative for 1/2-. In medium weight nuclei, then, J dependence appears promising, whereas no simple and informative rules have been clearly established for light nuclei.[134] At 30 MeV, e.g., Chant et al.[117] have done the (p,d) reaction on C^{12} and O^{16} with polarized protons. Almost all their data points for both 1/2- and 3/2- states show negative polarizations at angles up to 60°; the only point which is definitely positive and not consistent with zero asymmetry is for the 1/2- transition in O^{16} at 20°. The DWBA calculations for these data are in very poor agreement.

The J dependence of differential cross sections is well established in medium-weight nuclei for $\ell \leq 3$. The J dependence of the polarization can then be valuable spectroscopically in confirming these previous values and in assigning new ones in heavier nuclei where the cross sections do not give unambiguous information. Finally the explanations of J dependence of cross sections and polarization are not necessarily correlated, so that both data are needed as a test of the reaction model.

3. Structure Dependence

There remains the very interesting possibility that the J dependence of the differential polarization will be masked by an eventual nuclear structure dependence. Whereas the J dependence of the cross sections is a useful tool precisely because there seems to be little state dependence of the cross sections, this is not necessarily true of the polarization. The experimental capabilities are certainly adequate now to find such effects in transfer reactions similar to those which have already been found in inelastic scattering

to states of the same spin. While such a discovery would complicate the understanding of J dependence, it would provide definite impetus for a more realistic treatment of the form factor in DWBA calculations as outlined, e.g., by Pinkston and Satchler.[135] It could, then, lead to more fundamental information than J dependence.

4. The D State of the Deuteron

The spin-dependent terms which appear in the effective neutron-proton interaction can be included in the DWBA by keeping both S and D wave contributions to the deuteron wave function. This is an essential simplification over inelastic proton scattering where, e.g., $\underset{\sim}{\sigma}_i \cdot \underset{\sim}{\sigma}_j$ and tensor terms must be explicitly calculated. Johnson and Santos[136] have recently evaluated the influence of the D state on differential cross sections; its effects were found to be important for $\ell > 0$, and definitely necessary in the explanation of J dependence, e.g. The contributions to tensor polarization of the D state are large also. They have been able to account for the magnitudes[137] of the tensor polarization measured in Be^9(p,d) by Ivanovich et al.[105] although preliminary fits do not show good agreement in shape. On the other hand, D state effects are, surprisingly, not important in the analyses of the Wisconsin (d,p) asymmetry data.[138] Whether this is generally true for polarization data is not yet known.

The code of Johnson and Santos does not compute the effects of possible tensor potentials in the deuteron optical potential. The latter contributions do not modify the ℓ=0 first order relation (28), though they could have first-order effects for other ℓ values. There is little evidence that such terms are small,[61,63] yet their effects on the polarization distributions are unknown.

B) The Theories

1. DWBA

The number of careful DWBA analyses in which spin-orbit distortions were included in both proton and neutron channels is very limited. Good fits have been obtained for ℓ=0 transitions in the 2s-1d shell;[101] the asymmetry data from Wisconsin[119] have also been explained reasonably well. On the other hand, much less satisfactory results were obtained in the analyses of the ℓ=0 transition[128] in Sr^{88}(d,p) and the ℓ=1 transitions[117] in C^{12} and O^{16}. The results of a thorough study of the ℓ=3 ground state transition in Ca^{40}(d,p) at 14.3 MeV[125] were also disappointing, though there is apparently considerable energy dependence in the measured polarizations. In general the data are not sufficiently extensive or precise to provide a reasonable test of the DWBA.

2. New Reaction Models

A number of attempts to treat (d,p) reactions by three-body methods have appeared in recent years, and two of these have reached the stage of meaningful computation. Both the theory of Butler et al.,[139] and that of Coz and Pearson et al.[140] assume that the essential problem with the conventional DWBA is the treatment of the loosely-bound deuteron in many respects as an elementary particle inside the nucleus. The methods are formulated in such a way that neutron and proton optical potentials can be used instead of a deuteron optical potential.

The method of Coz and Pearson assumes the following physical picture. In a (d,p) reaction, as the deuteron passes near the nucleus, the proton is supposed to suddenly separate from the neutron and scatter from the nucleus as if the neutron were not present. In its most simple form, the theory

predicts that the differential cross section and polarization in a stripping reaction should be very similar, at large enough angles, to the corresponding quantities for elastically-scattered protons of the appropriate energy. However, more recent developments in the theory by Bang and Pearson[140] have placed more emphasis on the effects due to the captured neutron. No such simple physical interpretation of their method is given by Butler et al., and indeed it is the subject of some controversy.[140,141] Formal objections to both theories have also arisen.[141,142] However many of these objections can apparently now be resolved.[143,144] In particular, the interpretation of the spectroscopic factor in the Butler theory now seems to be well understood.[144,145]

Comparison with Experimental Data

Since both theories are still in the development stage, the predictions which have appeared are very limited in number and incorporate approximations which are not essential to the methods. An effective lower cutoff, e.g., appears in the calculations of Pearson et al. at a radius somewhat smaller than the nuclear radius. In the work of Butler et al., a residual contribution to the transition matrix from the asymptotic deuteron wave function has been neglected thus far. Improvement of these approximations can be expected to change the details of the Pearson type predictions more than those of Butler's. In particular, Butler's parameters are strictly determined by proton and neutron elastic scattering, as they should be. Bang and Pearson, however, allow themselves the liberty of changing the absorption depth in the neutron channel by a factor of two to make up for inadequacies in their approximation to the neutron capture contribution. Otherwise, both have used the optical parameters of Rosen[26] in all their calculations.

The following figures show polarization in (d,p) stripping predicted by both these models and the DWBA. The first (Fig. 13) illustrates three fits to the ℓ=0 transition in $Sr^{88}(d,p)Sr^{89}$ at a deuteron energy of 11.0 MeV; the fit obtained by Pearson et al.[146] is probably the best. For the ground-state ℓ=3 transition in $Ca^{40}(d,p)Ca^{41}$, shown in Fig. 14, we compare a DWBA fit to the 14.3 MeV data[125] with a fit to the 10.9 MeV results by the Butler group[139] and a fit to 10.0 and 10.9 MeV results by Pearson et al.[146] The predictions of both new models agree quite well with the experimental points, while the DWBA fits are rather poor. The latter are quite sensitive to the deuteron spin-orbit coupling; with more complete elastic scattering data and analyses, however, this in itself should no longer be a problem. It should be remarked here also that this is the one prediction shown by Pearson et al. in which the (d,p) polarization data do not bear a marked resemblance to the proton elastic polarization at large angles. The fact that their prediction resembles the data more than it resembles the elastic polarization indicates that their method cannot be dismissed by remarking on the difference between the experimental distributions of protons following (d,p) reactions and elastic scattering.

Other fits to polarization data with the new models have appeared but they cannot be directly compared. In general the quality of the fits is probably somewhat better than that obtained with the DWBA. Since only about ten pieces of data have been fit with each model and the experimental errors are large, this judgment is clearly subject to change. More extensive predictions of cross sections have appeared, and here the DWBA fits seem better than those obtained with the admittedly approximate forms of the new models published thus

far. Since a fit to the polarization without an equally good fit to the cross section is not meaningful, we must await many less approximate calculations from the new models before determining their usefulness.

CONCLUSION

The difficulties encountered in the preceding description of polarization phenomena in nuclear reactions have both experimental and theoretical origins. The first is due principally to the fact that very good polarized beams have appeared only recently. The second arises partly from the complexity of the subject and partly from the lack of motivation to refine programs which were already adequate to explain existing data. Now that precise experiments are being performed, the theoretical descriptions can also be expected to become more detailed. These efforts will undoubtedly lead to a much clearer understanding than is presently possible.

ACKNOWLEDGMENTS

We are deeply indebted to our many colleagues who sent preprints, reprints, and detailed descriptions of their work. We also acknowledge with gratitude our many helpful conversations with them.

REFERENCES

1. A. Abragam and J. M. Winter, Phys. Rev. Letters 1, 375 (1958); A. Abragam and J. M. Winter, Compt. Rend. 255, 1099 (1962).
2. R. Beurtey, Proceedings of the Second International Symposium on Polarization Phenomena of Nucleons, Karlsruhe 1965, ed. P. Huber and H. Schopper, (Birkhäuser Verlag, Basel, 1966), p. 33.
3. W. Haeberli, Annual Reviews of Nuclear Science, 17, 373, 1967.
4. Proceedings of the Second International Symposium on Polarization Phenomena of Nucleons, Karlsruhe 1965, ed. P. Huber and H. Schopper, (Birkhäuser Verlag, Basel, 1966).
5. J. M. Dickson, Progress in Nucl. Tech. and Instr. 1, 105 (1964).
6. R. Keller, CERN reports 3141/j and 60-2 (unpublished).
7. G. Clausnitzer, International Symposium on Polarization Phenomena of Nucleons, Basel 1960, ed. P. Huber and K. P. Meyer, (Berkhäuser Verlag, Basel, 1960).
8. H. F. Glavish, Proceedings of the Second International Symposium on Polarization Phenomena of Nucleons, Karlsruhe 1965, ed. P. Huber and H. Schopper, (Birkhäuser Verlag, Basel, 1966), p. 85; P. Birien, Nucl. Instr. and Methods, to be published.
9. R. Beurtey and J. Thirion, Nucl. Instr. and Methods 33, 338 (1965).
10. R. Beurtey and J. M. Durand, Nucl. Instr. and Methods, to be published.
11. W. P. Powell, Proceedings of the Second International Symposium on Polarization Phenomena of Nucleons, Karlsruhe 1965, ed. P. Huber and H. Schopper, (Birkhäuser Verlag, Basel, 1966), p. 47.
12. R. Beurtey, thesis, University of Paris, 1963, CEN-SACLAY report No. R2366 (unpublished).

13. J. Raynal, thesis, University of Paris, 1963, CEN-SACLAY report No. R2511 (unpublished).

14. R. C. Johnson, Nucl. Phys. 35, 654 (1962).

15. L. Rosen and J. E. Brolley, Phys. Rev. 107, 1454 (1957).

16. R. M. Craig et al., Nucl. Instr. and Methods 30, 269 (1964).

17. J. Arvieux, thesis, University of Grenoble, 1967.

18. G. Clausnitzer et al., Phys. Letters 25B, 267 (1967).

19. W. Haeberli, Proceedings of the Second International Symposium on Polarization Phenomena of Nucleons, Karlsruhe 1965, ed. P. Huber and H. Schopper, (Birkhäuser Verlag, Basel, 1966), p. 64; W. Haeberli et al., Phys. Rev. Letters 15, 267, (1965); W. Grübler et al., Phys. Letters 24B, 280 (1967); W. Grübler et al., Phys. Letters 24B, 335 (1967).

20. T. K. Khoe and L. C. Teng, CERN report no. 6319, 118 (1963) (unpublished).

21. E. K. Zavoiskii, Soviet Physics JETP 5, 603 (1957).

22. B. Donally, T. Clapp, W. Sawyer, and M. Schultz, Phys. Rev. Letters 12, 502 (1964).

23. B. Donally and W. Sawyer, Proceedings of the Second International Symposium on Polarization Phenomena of Nucleons, Karlsruhe 1965, ed. P. Huber and H. Schopper, (Birkhäuser Verlag, Basel, 1966), p. 64.

24. P. Schwandt, Bull. Am. Phys. Soc., to be published.

25. G. C. Phillips, Proceedings of the Paris Conference on Polarized Targets and Polarized Ion Sources, Paris, 1966.

26. L. Rosen, Proceedings of the Second International Symposium on Polarization Phenomena of Nucleons, Karlsruhe 1965, ed. P. Huber and H. Schopper, (Birkhäuser Verlag, Basel, 1966), p. 253.

27. J. D. Steben and M. K. Brussel, Phys. Rev. 146, 780 (1966).

28. D. J. Baugh, J. A. R. Griffith, and S. Roman, Nucl. Phys. 83, 481 (1966).

29. P. Kossanyi-Demay, R. de Swiniarski, and C. Glashausser, Nucl. Phys. A94, 513 (1967).

30. C. Glashausser, P. Kossanyi-Demay, and R. de Swiniarski, J. Phys. (France), to be published.

31. R. M. Craig, J. C. Dore, G. W. Greenlees, J. Lowe, and D. L. Watson, Nucl. Phys. 79, 177 (1966).

32. J. Lowe and D. L. Watson, Phys. Letters 23, 261 (1966).

33. Hudson B. Eldridge, thesis, University of California at Los Angeles, 1967, (unpublished).

34. D. L. Watson, J. Lowe, J. C. Dore, R. M. Craig, and D. J. Baugh, Nucl. Phys. A92, 193 (1967).

35. G. R. Satchler, Nucl. Phys. A92, 273 (1967).

36. G. W. Greenlees and G. J. Pyle, Phys. Rev. 149, 136 (1966).

37. L. N. Blumberg, E. E. Gross, A. van der Woude, A. Zucker, and R. H. Bassel, Phys. Rev. 147, 812 (1966).

38. M. P. Fricke, E. E. Gross, B. J. Morton, and A. Zucker, Phys. Rev. 156, 1207 (1967).

39. T. A. Cahill, J. R. Richardson, and R. P. Haddock, Phys. Rev. 144, 932 (1966).

40. R. M. Craig, J. C. Dore, J. Lowe, and D. L. Watson, Nucl. Phys. 86, 113 (1966).

41. V. E. Lewis, E. J. Burge, A. A. Rush, and D. A. Smith, Nucl. Phys. A101, 589 (1967).

42. Edmund T. Boschitz, Phys. Rev. Letters 17, 97 (1967).

43. L. J. B. Goldfarb, G. W. Greenlees, and M. B. Hooper, Phys. Rev. 144, 829 (1966).

44. L. H. Thomas, Nature 117, 514 (1926).

45. D. A. Lind, D. E. Heagerty, and J. G. Kelly, Bull. Am. Phys. Soc. 2, 104 (1965).

46. G. W. Greenlees, G. J. Pyle, and Y. C. Tang, Phys. Rev. Letters 17, 33 (1966).

47. W. Heisenberg, Theorie des Atomkernes (Max-Planck Institut für Physik, Göttingen, 1951), p. 22.

48. G. E. Brown, Proc. Phys. Soc. (London) 70A, 361 (1957).

49. S. Fernbach, W. Heckrotte, and J. Lepore, Phys. Rev. 97, 1059 (1955); R. J. Blin-Stoyle, Phil. Mag. 46, 973 (1955); H. S. Köhler, Nucl. Phys. 9, 49 (1958).

50. H. C. Volkin, Bull. Am. Phys. Soc. 9, 439 (1964).

51. Donald W. L. Sprung and P. C. Bhargava, Phys. Rev. 156, 1185 (1967).

52. M. B. Hooper, private communication.

53. G. W. Greenlees et al., Nucl. Phys. 49, 496 (1963).

54. J. L. Adams, W. J. Thompson, and D. Robson, Nucl. Phys. 89, 377 (1966).

55. C. F. Moore and G. E. Terrell, Phys. Rev. Letters 16, 804 (1966).

56. L. Veeser, J. Ellis, and W. Haeberli, Phys. Rev. Letters 18, 1063 (1967).

57. G. R. Satchler, Nucl. Phys. 21, 116 (1960).

58. S. Watanabe, Nucl. Phys. 8, 484 (1958).

59. R. Beurtey et al., Compt. Rend. 256, 922 (1963).

60. J. Arvieux, T. Cahill, J. Goudergues, H. Krug, B. Mayer, and A. Papineau, J. Phys. (France), to be published.

61. P. Schwandt, private communication.

62. J. Arvieux et al., Phys. Letters 16, 149 (1965).

63. J. Raynal, Phys. Letters 7, 281 (1963).

64. J. Hufner and A. de Shalit, Phys. Letters 15, 52 (1965).

65. E. F. Gibson, B. W. Ridley, J. J. Kraushaar, M. E. Rickey, and R. H. Bassel, Phys. Rev. 155, 1194 (1967).

66. W. E. Burcham et al., Compt. Rend. Congrès Int. Phys. Nucl., Paris, 1964, p. 877.

67. W. E. Frahn and G. Wiechers, Nucl. Phys. 74, 65 (1965).

68. J. Beery, private communication.

69. P. Darriulat, J. M. Fowler, R. de Swiniarski, and J. Thirion, Proceedings of the Second International Symposium on Polarization Phenomena of Nucleons, Karlsruhe 1965, ed. P. Huber and H. Schopper, (Birkhäuser Verlag, Basel, 1966), p. 342.

70. C. Glashausser, R. de Swiniarski, J. Thirion, and A. D. Hill, Phys. Rev. 164, 1437 (1967).

71. A. G. Blair, C. Glashausser, J. Goudergues, R. M. Lombard, B. Mayer, R. de Swiniarski, J. Thirion, and P. Vaganov, Proc. Int. Nucl. Phys. Conf., Tokyo, 1967.

72. R. M. Craig, J. C. Dore, G. W. Greenlees, J. Lowe, and D. L. Watson, Nucl. Phys. 83, 493 (1966).

73. J. Lowe, private communication.

74. D. J. Baugh, M. J. Kenny, J. Lowe, D. L. Watson, and H. Wojciechowski, Nucl. Phys. A99, 203 (1967).

75. M. P. Fricke, E. E. Gross, and A. Zucker, to be published in Phys. Rev.; M. P. Fricke, R. M. Drisko, R. H. Bassel, E. E. Gross, B. J. Morton, and A. Zucker, Phys. Rev. Letters 16, 746 (1966).

76. D. L. Hendrie, N. K. Glendenning, B. G. Harvey, O. N. Jarvis, H. H. Duhm, J. Saudinos, and J. Mahoney, Phys. Letters 26B, 127 (1968).

77. A. D. Hill, unpublished notes.

78. G. R. Satchler, Nucl. Phys. 55, 1 (1964).

79. J. Blair and H. Sherif, to be published.

80. S. F. Eccles, H. F. Lutz, and V. A. Madsen, Phys. Rev. 141, 1067 (1966).

81. N. K. Glendenning and M. Veneroni, Phys. Rev. 144, 839 (1966).

82. G. R. Satchler, Nucl. Phys. 77, 481 (1966).

83. G. R. Satchler, Nucl. Phys. A95, 1 (1967).

84. A. Faessler, N. K. Glendenning, and A. Plastino, Phys. Rev. 159, 846 (1967).

85. W. G. Love and G. R. Satchler, Nucl. Phys. A101, 424 (1967).

86. N. K. Glendenning, Lectures at the Enrico Fermi Summer School, Varenna, 1967, UCRL report no. 17503.

87. J. D. Anderson, Proc. Conf. on Isobaric Spin, 1966, (Academic Press, New York, 1966), p. 530.

88. B. D. Walker, C. Wong, J. D. Anderson, J. W. Mc Clure, and R. W. Bauer, Phys. Rev. 137, B347 (1965); B. D. Walker, C. Wong, J. D. Anderson, and J. W. Mc Clure, Phys. Rev. 137, B1504 (1965).

89. M. Fricke, thesis, University of Minnesota, 1967 (unpublished); G. R. Satchler, private communication.

90. G. R. Satchler, Phys. Letters 19, 312 (1965).

91. R. Ballini, N. Cindro, J. Delaunay, J. Fouan, M. Loret, and J. P. Passerieux, Nucl. Phys. A97, 561 (1967).

92. W. A. Kolasinski, thesis, University of Washington, 1967 (unpublished).

93. K. A. Amos, V. A. Madsen, and I. E. Mc Carthy, Nucl. Phys. A94, 103 (1967).

94. V. A. Madsen, private communication.

95. P. H. Stelson, R. L. Robinson, H. J. Kim, J. Rapaport, and G. R. Satchler, Nucl. Phys. 68, 97 (1965).

96. S. T. Butler, Proc. Roy. Soc. 208, A559 (1951).

97. J. A. Green and W. C. Parkinson, Phys. Rev. 127, 926 (1962).

98. B. Hird, J. Cookson, and M. S. Bokhari, Proc. Phys. Soc. (London) 72, 489 (1958).

99. R. G. Allas, R. W. Bercaw, and F. B. Shull, Phys. Rev. 127, 1252 (1962).

100. G. F. Nemets, M. V. Pasechnik, and N. N. Purcherov, Nucl. Phys. 45, 1 (1963).

101. L. H. Reber and J. X. Saladin, Phys. Rev. 133, B1155 (1964).

102. E. T. Boschitz and J. S. Vincent, NASA report no. R-218 (unpublished).

103. B. Hird and A. Strazalkowski, Proc. Phys. Soc. 75, 868 (1960).

104. S. E. Darden and A. J. Froelich, Phys. Rev. 140, B69 (1965).

105. M. Ivanovich, H. Cords, and G. U. Din, Nucl. Phys. A97, 177 (1967).

106. J. C. Hensel and W. C. Parkinson, Phys. Rev. 110, 128 (1958).

107. R. W. Bercaw and F. B. Shull, Bull. Am. Phys. Soc. 7, 269 (1962).

108. M. Takeda, S. Kato, C. Hu, and N. Takahashi, in Proceedings of the Int. Conf. on Nucl. Structure, Kingston, Ontario, 1960 (University of Toronto Press, Toronto, 1960).

109. Donald G. Simons, Phys. Rev. 155, 1132 (1967); D. G. Simons and R. W. Detenbeck, Phys. Rev. 137, B1471 (1965); Donald G. Simons, private communication.

110. M. S. Bokhari, J. A. Cookson, B. Hird, and B. Wessakul, Proc. Phys. Soc. (London) 72, 88 (1958).

111. R. G. Allas and F. B. Shull, Phys. Rev. 116, 996 (1959).

112. W. P. Johnson and D. W. Miller, Phys. Rev. 124, 1190 (1961).

113. A. C. Juveland and W. Jentscke, Phys. Rev. 110, 456 (1958).

114. A. Isoya, S. Micheletti, and L. H. Reber, Phys. Rev. 128, 806 (1962).

115. J. E. Evans, J. A. Kuehner, and E. Almqvist, Phys. Rev. 131, 1632 (1963).

116. R. Beurtey et al., Conference on Direct Interactions and Nuclear Reaction Mechanisms, E. Clementel and C. Villi, ed., Gordon and Breach (New York), 1963, p. 619.

117. N. S. Chant, P. S. Fisher, and D. K. Scott, Nucl. Phys. A99, 669 (1967).

118. J. E. Evans, Phys. Rev. 131, 1642 (1963).

119. T. Yule and W. Haeberli, Phys. Rev. Letters 19, 756 (1967).

120. A. Isoya and M. J. Marrone, Phys. Rev. 128, 800 (1962).

121. R. Beurtey, R. Chaminade, A. Falcoz, R. Maillard, T. Mikumo, A. Papineau, L. Schecter, and J. Thirion, J. Phys. (France) 24, 1038 (1963).

122. R. W. Bercaw and F. B. Shull, Phys. Rev. 133, B632 (1964).

123. S. Kato, N. Takahashi, M. Tahida, T. Yamazaki, and S. Yasukawa, Osaka University Report no. OU-LNS 64-2, 1964 (unpublished).

124. M. V. Pasechnik, L. S. Saltykov, and D. I. Tambovtzev, Zh. Eksperim. i Teor. Fiz. 43, 1575 (1963) [English translation: Soviet Phys. - JETP 16, 1111 (1963)].

125. Sven A. Hjorth, J. X. Saladin, and G. R. Satchler, Phys. Rev. 138, B1425 (1965).

126. N. S. Chant, private communication.

127. A. A. Rollefson, P. F. Brown, J. A. Burke, P. A. Crowley, and J. X. Saladin, Phys. Rev. 154, 1088 (1967).

128. E. J. Ludwig and D. W. Miller, Phys. Rev. 138, B364 (1965).

129. M. B. Hooper, Nucl. Phys. 76, 449 (1966).

130. R. C. Johnson, Nucl. Phys. A90, 289 (1967).

131. H. C. Newns, Proc. Phys. Soc. A66, 477 (1953).

132. D. F. Walls, Nucl. Phys. A90, 353 (1967).

133. S. T. Butler, Proceedings of the Rutherford Jubilee Conference, Manchester, 1961 (Heywood and Co., Ltd., London, 1962), p. 492.

134. D. W. Miller, Proceedings of the Second International Symposium on Polarization Phenomena of Nucleons, Karlsruhe 1965, ed. P. Huber and H. Schopper, (Birkhäuser Verlag, Basel, 1966), p. 410.

135. W. T. Pinkston and G. R. Satchler, Nucl. Phys. 72, 641 (1965).

136. R. C. Johnson and F. D. Santos, Phys. Rev. Letters 19, 364 (1967).

137. R. C. Johnson, private communication.

138. R. C. Johnson, private communication from W. Haeberli.

139. S. T. Butler, Nature 207, 1346 (1965); S. T. Butler, R. G. Hewitt, and R. M. May, Phys. Rev. Letters 26, 1033 (1965); S. T. Butler, R. G. L. Hewitt, B. H. J. Mc Kellar and R. M. May, Ann. Physics 43, 282 (1967); R. M. May and J. S. Truelove, Ann. Physics 43, 322 (1967).

140. C. A. Pearson and M. Coz, Nucl. Phys. 82, 533 (1966); C. A. Pearson and M. Coz, Nucl. Phys. 82, 545 (1966); C. A. Pearson and M. Coz, Ann. Phys. 39, 199 (1966); C. A. Pearson and E. H. Auerbach, Phys. Letters 20, 418 (1966); J. M. Bang and C. A. Pearson, Nucl. Phys. A100, 1 (1967); J. M. Bang, C. A. Pearson, and L. Pocs, Nucl. Phys. A100, 24 (1967).

141. C. F. Clement, Phys. Rev. Letters 17, 760 (1966).

142. F. S. Levin, Nuovo Cimento IL B, N. 2, 200 (1967).

143. I. E. Mc Carthy, to be published.

144. C. F. Clement, Phys. Rev. Letters 20, 22 (1968).

145. S. T. Butler, R. G. L. Hewitt, and J. S. Truelove, Phys. Letters 26B, 264 (1968); and Phys. Letters 26B, 267 (1968).

146. C. A. Pearson, private communication.

Table I. Polarization measurements and optical model analyses of elastic scattering. The optical parameters given are either the average geometrical parameters derived by the authors or, if no average set was used, the average of the best fit parameters determined. The parameters are defined by Eq. (14).

E_p (MeV)	Target Nuclei	Optical Parameters r_o	a_o	r_I	a_I	r_{so}	a_{so}	Reference
8.2-11.4	N^{14}	-	-	-	-	-	-	27
12.8-13.4	C^{12}	-	-	-	-	-	-	27
17.8	Be,S,Fe,Co,Cu, Zn,Ga,Ag,In	1.25	0.65	1.25	0.47	1.04	0.65	28
18.6	$Ti^{48,50}$,Cr^{52},$Fe^{54,56}$ $Ni^{58,62,64}$,Cu^{63}	1.25	0.65	1.25	0.47	1.12	0.47	29
		1.10	0.75	1.30	0.55	1.0	0.55	30
20-29	C^{12}	Analysis includes three compound nucleus resonances						31,32
24-40	O^{16}	-	-	-	-	-	-	33
26.3	Ca,Ni^{58},Pb^{208}	1.12	0.75	1.33	0.58	1.12	0.75	34
		1.20	0.70	1.20	0.70	1.10	0.70	34
30	Ca^{40},Ni^{58},Co^{59}, Ni^{60},Sn^{120},Pb^{208}	1.12	0.75	1.33	0.58	1.12	0.75	35
		1.20	0.70	1.20	0.70	1.10	0.70	36
30	Ca,Ni^{58},Ni^{60},Pb^{208}	extension of previous measurements and analyses to back angles						34
40	C^{12},Ca^{40},Ni^{58},Zr^{90} Pb^{208}	1.18	0.70	1.30	0.60	1.05	0.70	37
40	Si^{28},Fe^{54},Co^{59},Ni^{60} Zn^{68},Sn^{120},C^{12}, Ca^{40},Ni^{58},Zr^{90},Pb^{208}	1.16	0.75	1.37	0.63	1.06	0.74	38
45	Be,C,Al,V,Rh	-	-	-	-	-	-	39
49	Ca,Ni^{58},Ni^{60},Pb^{208}	-	-	-	-	-	-	40
50	Mg^{24}	1.1	0.73	1.29	0.60	1.0	0.58	41
	Zn^{64}(Zn^{68})	1.1	0.82	1.29	0.62	1.0	0.66	41

Table II. Measurements of polarization parameters in the inelastic scattering of protons. The orbital angular momentum transfer is indicated by ℓ.

Target	E_p (MeV)	Ref.
A. $\ell=2$		
C^{12}, Ni^{60}, Ni^{62}	16.5	69
$Ti^{48,50}, Cr^{52}, Fe^{54,56}$ $Ni^{58,62,64}, Cu^{63}$	18.6	70
$Mg^{24,25,26}, Al^{27}, Si^{28}$ $Zr^{90,92}, Mo^{92}$	20.0	71
C^{12}, Si^{28}	29.0	72
Be^{9}	30.3	73
Fe^{54}	30.4	74
$Si^{28}, Fe^{54}, Ni^{58,60}$	40.0	75
C^{12}, Si^{28}	49.0	72
$Mg^{24}, Zn^{64,68}$	50.0	41
B. $\ell=3$		
$Fe^{54,56}, Ni^{58,62}$	18.6	70
$Ca^{40}, Zr^{90,92}, Mo^{92}$	20.0	71
$Si^{28}, Fe^{54}, Ni^{58,60}$	40.0	75
C. $\ell=4$		
Fe^{54}, Ni^{58}	18.6	70
Mg, Si, Zr, Mo	20.0	71

Table III. Polarization measurements in transfer reactions. Measurements of the asymmetry following reactions initiated by polarized particles are marked (A).

Reaction	$E_{inc.}$	Transition	Ref.
$Be^9(d,p)Be^{10}$	7.8,8.9,10.0 13.6,15.0,20.6	$3/2- \rightarrow 0^+$	97,98,99,100,101, 102
$Be^9(d,p)Be^{10}$	6.0,15.0,20.6	$3/2- \rightarrow 2^+$	101,102,103
$Be^9(p,d)Be^8$	2.6,3.7,4.91, 6.90,8.27,9.80	$3/2- \rightarrow 0^+$	104,105
$B^{10}(d,p)B^{11}$	7.8,8.9,10.0, 11.4,13.6,21.0	$3^+ \rightarrow 3/2-$	98,100,102,106,107, 108
$B^{10}(He^3,p)C^{12}$	1.75 - 2.8	$0^+ \rightarrow 2^+$	109
$C^{12}(d,p)C^{13}$	6.9,7.8,8.9,10.0, 10.8,11.8,11.9, 15.0,21.0,22.0(A)	$0^+ \rightarrow 1/2-$	98,106,110,111,112 113,114,115,116
$C^{12}(d,p)C^{13}$	5 - 10, 15	$0^+ \rightarrow 1/2^+$	101,115
$C^{12}(p,d)C^{11}$	30(A)	$0^+ \rightarrow 1/2-,3/2-,7/2-$	117
$O^{16}(d,p)O^{17}$	9.55	$0^+ \rightarrow 1/2^+$	118
$O^{16}(p,d)O^{15}$	30(A)	$0^+ \rightarrow 1/2-,3/2-,$	117
$Mg^{24}(d,p)Mg^{25}$	8.0(A),15.0	$0^+ \rightarrow 5/2^+,3/2^+,1/2^+$	101,119

Table III (Continued)

Reaction	$E_{inc.}$	Transition	Ref.
$Si^{28}(d,p)Si^{29}$	100,15.0,21.0, 22.0(A)	$0^+ \rightarrow 1/2^+$, $0^+ \rightarrow 3/2^+$	102,107,120,121
$Ca^{40}(d,p)Ca^{41}$	7.0(A),10.0,10.9, 11.4,13.8,14.3, 21.0	$0^+ \rightarrow 1/2-,3/2-,7/2-$	108,119,122,123, 124,102,125
$Ca^{40}(p,d)Ca^{39}$	30(A)	$0^+ \rightarrow 3/2^+,5/2^+,1/2^+$	126
$V^{51}(d,p)V^{52}$	15.0	$0^+ \rightarrow 3/2-$	114
$Cr^{52}(d,p)Cr^{53}$	8.0(A)	$0^+ \rightarrow 5/2-,3/2-,1/2-$	119
$Ni^{58}(d,p)Ni^{59}$	15.0	$0^+ \rightarrow 1/2-,3/2-$	127
$Sr^{88}(d,p)Sr^{89}$	11.0	$0^+ \rightarrow 1/2^+$	128

FIGURE CAPTIONS

Fig. 1. Rabi diagram for atomic hydrogen showing the energy levels as a function of external magnetic field. The magnetic field is labeled by X, where X is (H/507)G, and ΔE is 5.82×10^{-6} eV. The magnetic quantum numbers m_F, m_I, and m_J refer to the spins of the atom, the proton, and the electron, respectively.

Fig. 2. Rabi diagram for atomic deuterium. The magnetic field is now given in units of (H/117)G, and ΔE is 1.34×10^{-6} eV. The magnetic quantum number m_I now refers to the deuteron; m_F and m_J refer to the atom and the electron respectively.

Fig. 3. Rabi diagram for the $2S_{1/2}$ and $2P_{1/2}$ states in atomic hydrogen. The two states are separated by the Lamb shift (4.38×10^{-6} eV).

Fig. 4. Polarization as a function of incident energy in the elastic scattering of protons from Ce^{140} at 80° and 109°. The solid lines are theoretical curves. The resonance energies and ℓ values for the analog states in Pr^{141} are shown at the bottom. Near the third resonance, the dashed curve is for spin 1/2 and the solid curve for spin 3/2.

Fig. 5. Vector polarization (it_{11}) in the elastic scattering of 22-MeV deuterons from Zr^{90} and Pb^{208}. The data were taken at Saclay (Ref. 60). The solid curves are visual guides.

Fig. 6. Tensor polarization parameters ($Q = \frac{1}{2\sqrt{2}} (t_{20} + \sqrt{6}\, t_{22})$ for the elastic scattering of 22-MeV deuterons from Ni^{60}, Zr^{90}, and Pb^{208}. The data were taken at Saclay (Ref. 60).

Fig. 7. Polarization of 29-MeV He^3 ions elastically scattered from C(top), Sn(center), and Au(bottom). The measurements were made by Burcham et

al. (Ref. 66). The curves are theoretical fits by Frahn and Wiechers (Ref. 67).

Fig. 8. Asymmetry in the inelastic scattering of 20-MeV polarized protons. The curves have been drawn through data points which were measured every 5° with errors generally of ±0.03. (Ref. 71). Representative points are shown.

Fig. 9. Comparison of theoretical prediction with asymmetry data in the inelastic scattering of 18.6-MeV (Ref. 70) and 40-MeV (Ref. 75) protons. The four types of coupling used to compute the form factor are noted in the legend. Note that the scales for the two energies are not the same.

Fig. 10. Asymmetry data (Ref. 70) and theoretical predictions (Ref. 83) for the first two 2^+ states in Fe^{54}; the incident proton energy is 18.6 MeV. The solid curves use an optical potential with independent spin-orbit coupling parameters, while the dashed curve for the 1.41-MeV level uses a potential which gives an optimum fit to elastic scattering cross sections but with constrained spin-orbit coupling. The ground and first excited state were taken to be $(f_{7/2}^{-2})$ configurations, while an $(f_{7/2}^{-3} p_{3/2})$ configuration was assumed for the 2.97-MeV excitation with V_1=0(solid curve), $V_1 = \frac{1}{2}V_o$ (dashed curve), and $V_1 = -\frac{1}{2}V_o$ (dotted curve) (see Eq. (26)).

Fig. 11. Comparison of the polarization measurements on $Mg^{24}(d,p)Mg^{25*}$(0.58 MeV), $Al^{27}(d,p)Al^{28}$(g.s.), and $Si^{28}(d,p)Si^{29}$(g.s.) at 15 MeV (Ref. 101) with distorted wave calculations by Bassel, Drisko, Johnson, and Satchler.

Fig. 12. The vector analyzing power $P_d(\theta)$ for various (d,p) reactions measured by the Wisconsin group (Ref. 119). The solid (open) symbols are for $j = \ell - \frac{1}{2}$ ($\ell + \frac{1}{2}$) transitions. For $\ell = 1$, the solid (dashed) curve is a DWBA calculation for the J = 1/2, 3.95-MeV (J = 3/2, 1.95-MeV) state in Ca^{41} for an incident deuteron energy of 7.0 MeV. For $\ell = 2$, the solid curve is the DWBA prediction for the J = 3/2, 1.28-MeV state in Si^{29} at a deuteron energy of 10 MeV, while the dashed curve assumes that J is 5/2. The solid (dashed) curve for the $\ell = 3$ transitions is for the J = 5/2, 0.39-MeV (J = 7/2, 0.0-MeV) state in $Ni^{59}(Ca^{41})$ for an incident energy of 10.0 (7.0) MeV.

Fig. 13. Calculated and measured polarizations for $Sr^{88}(d,p)Sr^{89}$ (Q = 3.11 MeV, $\ell = 0$, E_d = 11 MeV). The data were taken by Ludwig and Miller.[128] The curves at the top are the predictions of Pearson et al. (Ref. 140). The parameters of Rosen were used except that $W_n = 2\ W_n$ Rosen (solid curve) and $W_n = 4\ W_n$ Rosen (broken curve). The dotted curve is the proton elastic polarization with Rosen parameters. The predictions of Butler for the same data are shown in the center and the shaded band at the bottom represents a range of possible DWBA predictions (Ref. 134). The lower figure also shows the data and DWBA calculations for the (d,p) differential cross sections.

Fig. 14. Calculated and measured polarizations for the $Ca^{40}(d,p)Ca^{41}$ ground state (ℓ=3) reaction. The upper curves show fits by Pearson et al.[146] at 10.9 MeV (broken curve) and 12 MeV (solid curve) to the combined 10- and 10.9-MeV data. Rosen parameters were used except that: $W_n = W_D$ (Rosen surface) + W_s (Rosen volume). At the center, the fits of Butler's

group[139] to the 10.9-MeV data are shown. The lowest curves are three DWBA fits to the 14.3-MeV data, with real (2), imaginary (3), and no (1) deuteron spin-orbit term (Ref. 124).

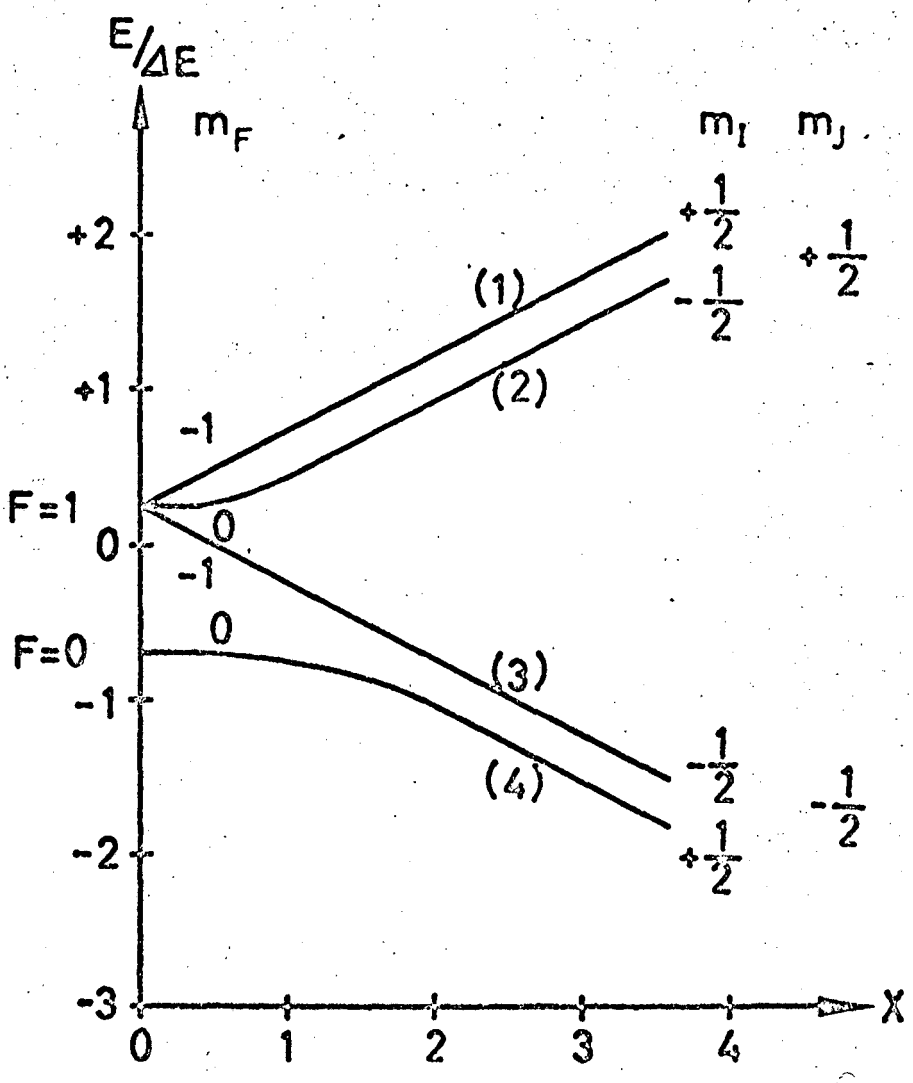

XBL 6711-6008

Fig. 1.

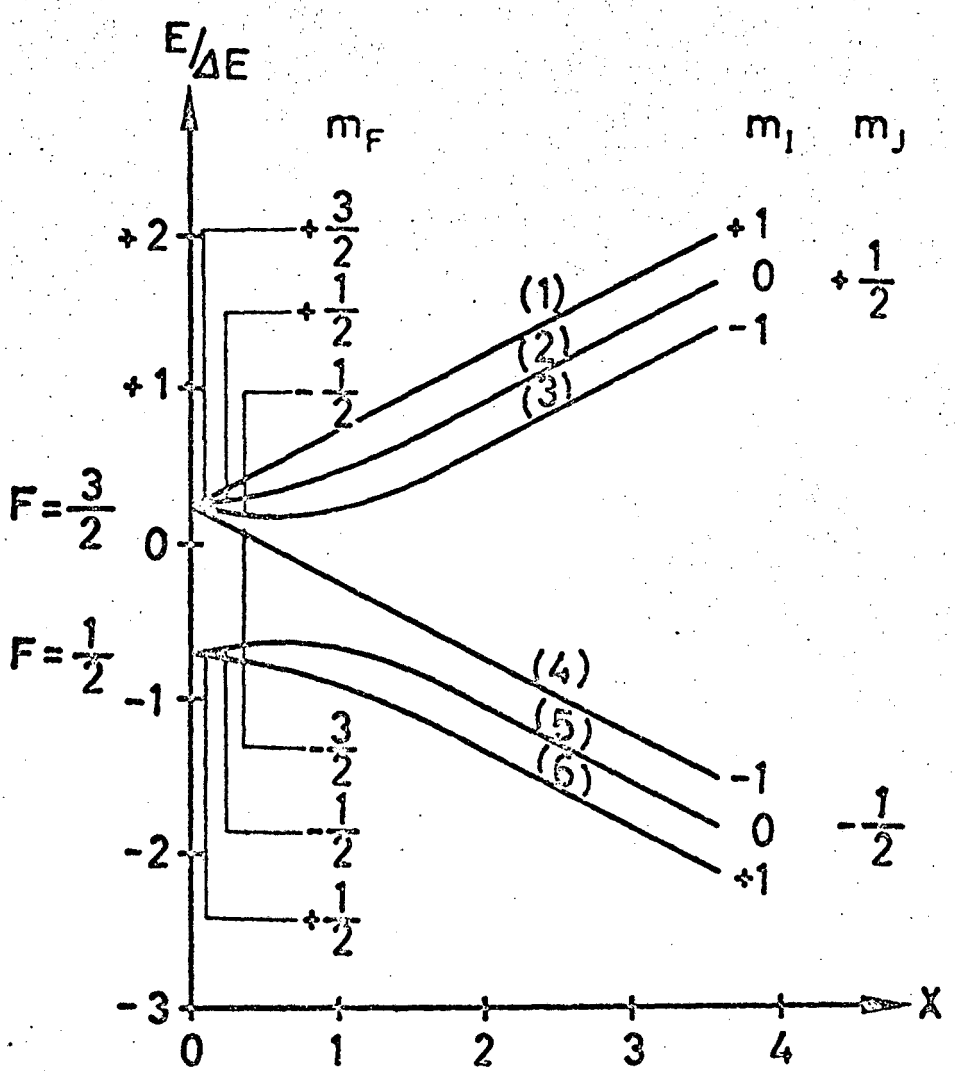

XBL 6711-6009

Fig. 2.

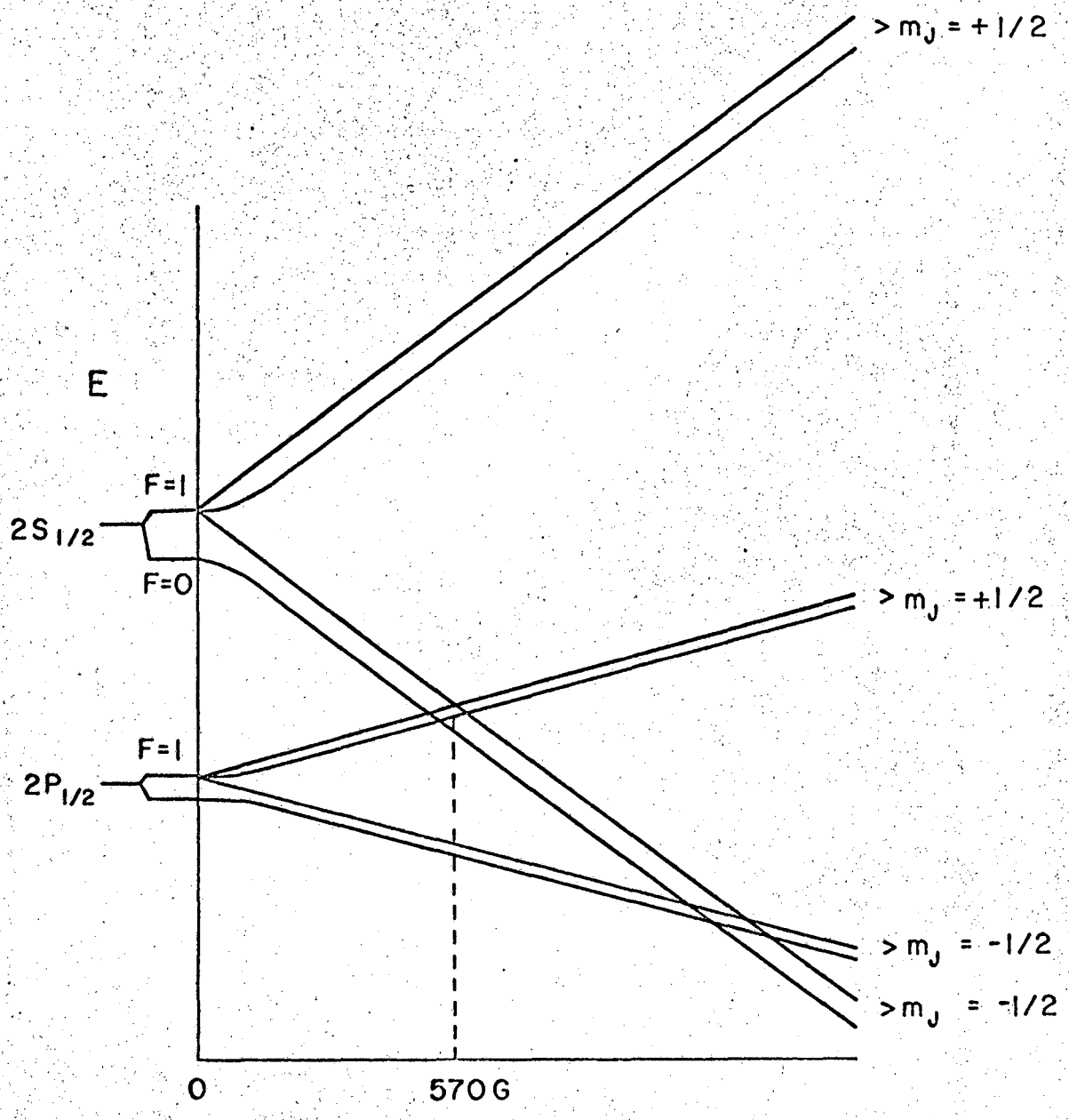

Fig. 3.

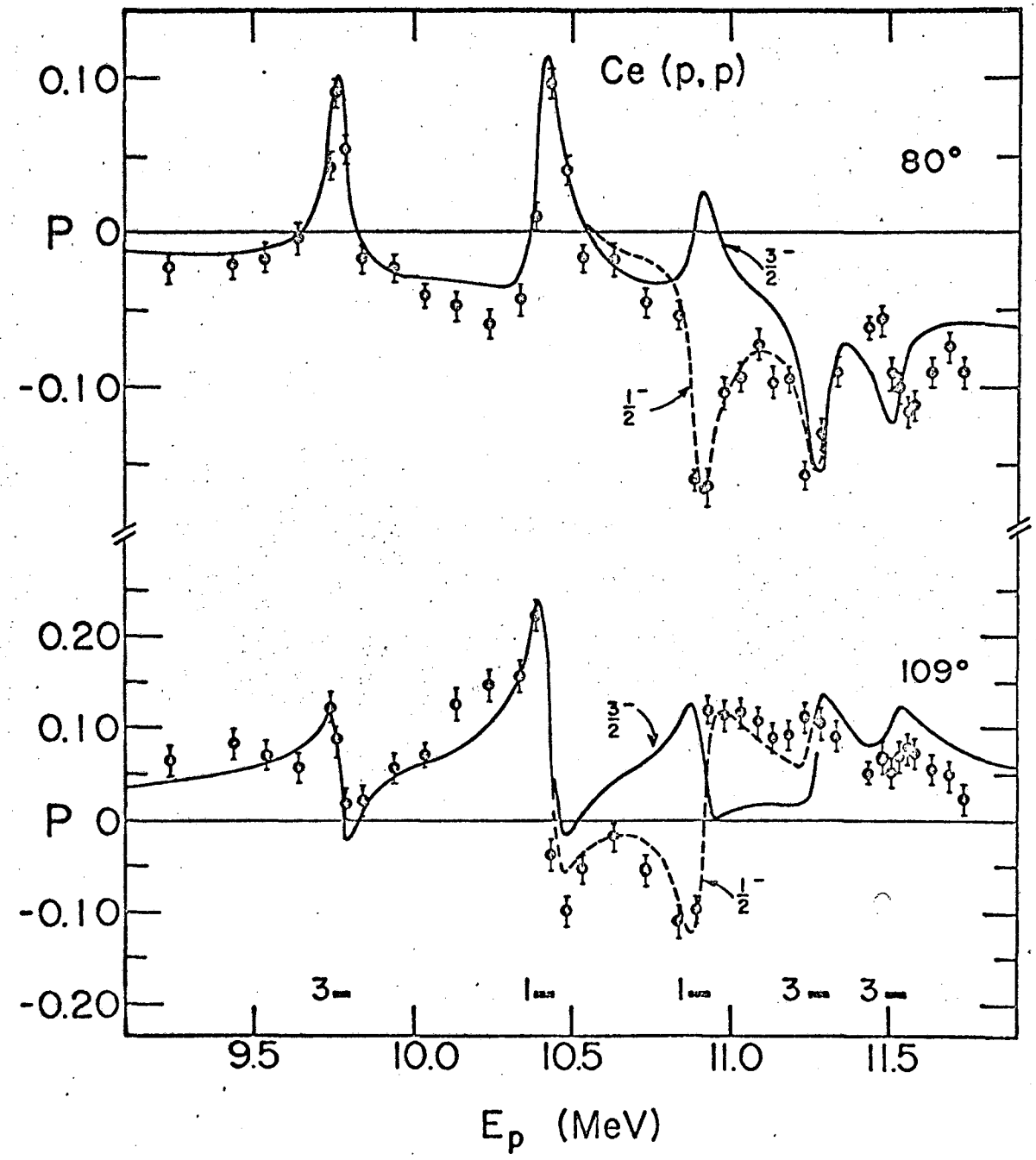
Ce (p, p)
80°
109°
0.10
P 0
-0.10
0.20
-0.20
3/2⁻
1/2⁻
3/2⁻
1/2⁻
3
1
1
3
3
9.5
10.0
10.5
11.0
11.5
Ep (MeV)
XBL 6711-6093

Fig. 4.

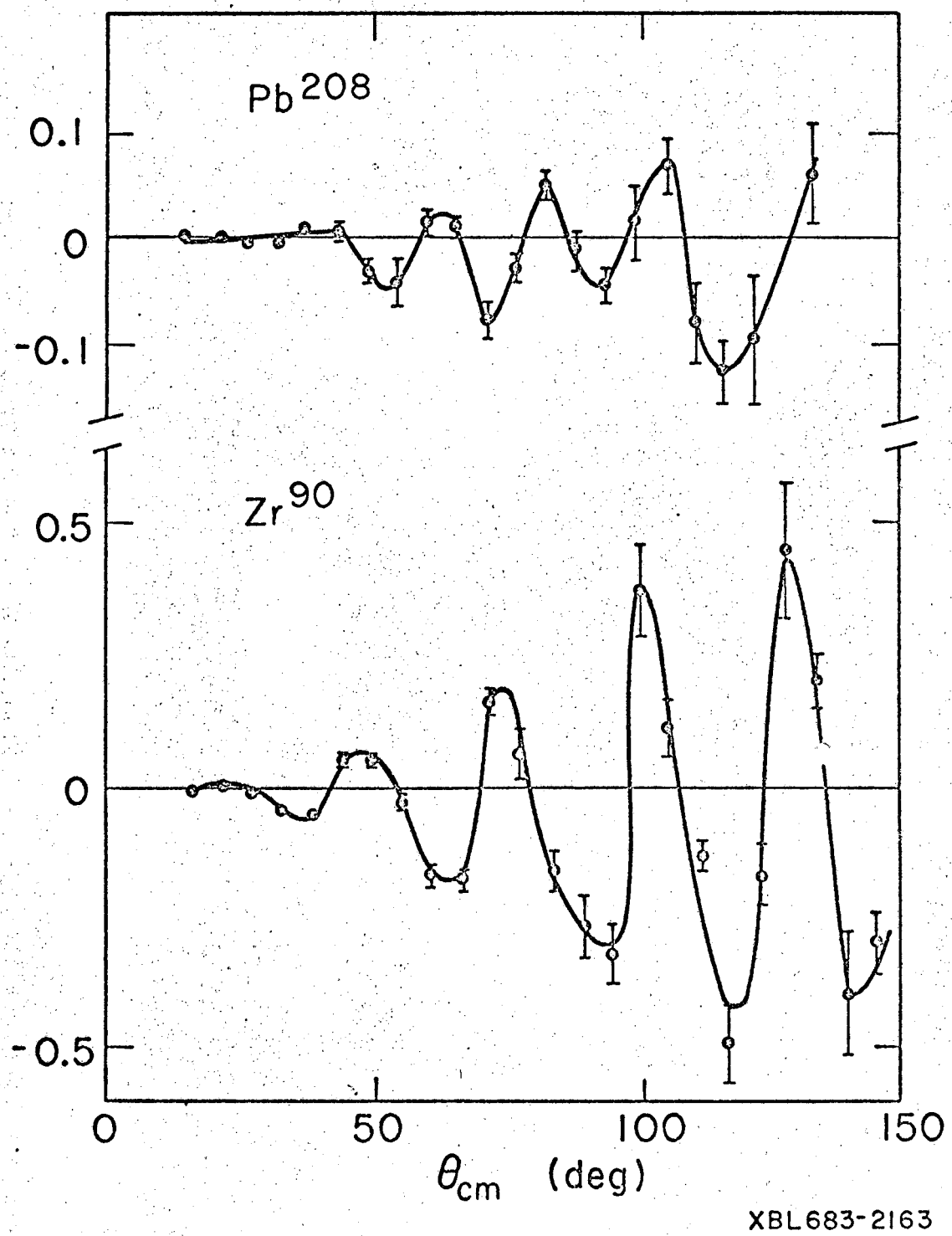

Fig. 5.

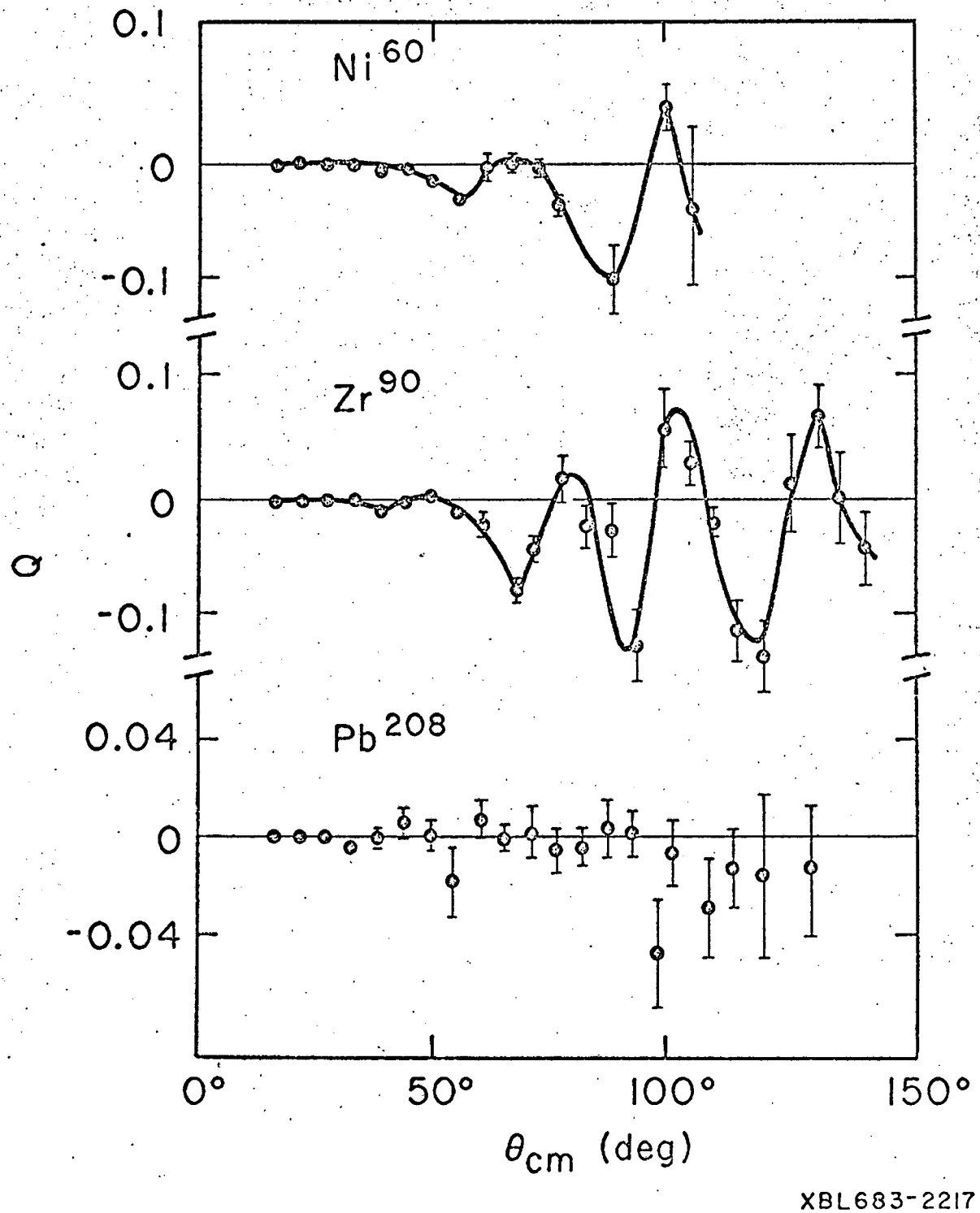
0.1
Ni 60
0
-0.1
0.1
Zr 90
0
-0.1
σ
0.04
Pb 208
0
-0.04
0°
50°
100°
150°
θcm (deg)
XBL683-2217

Fig. 6.

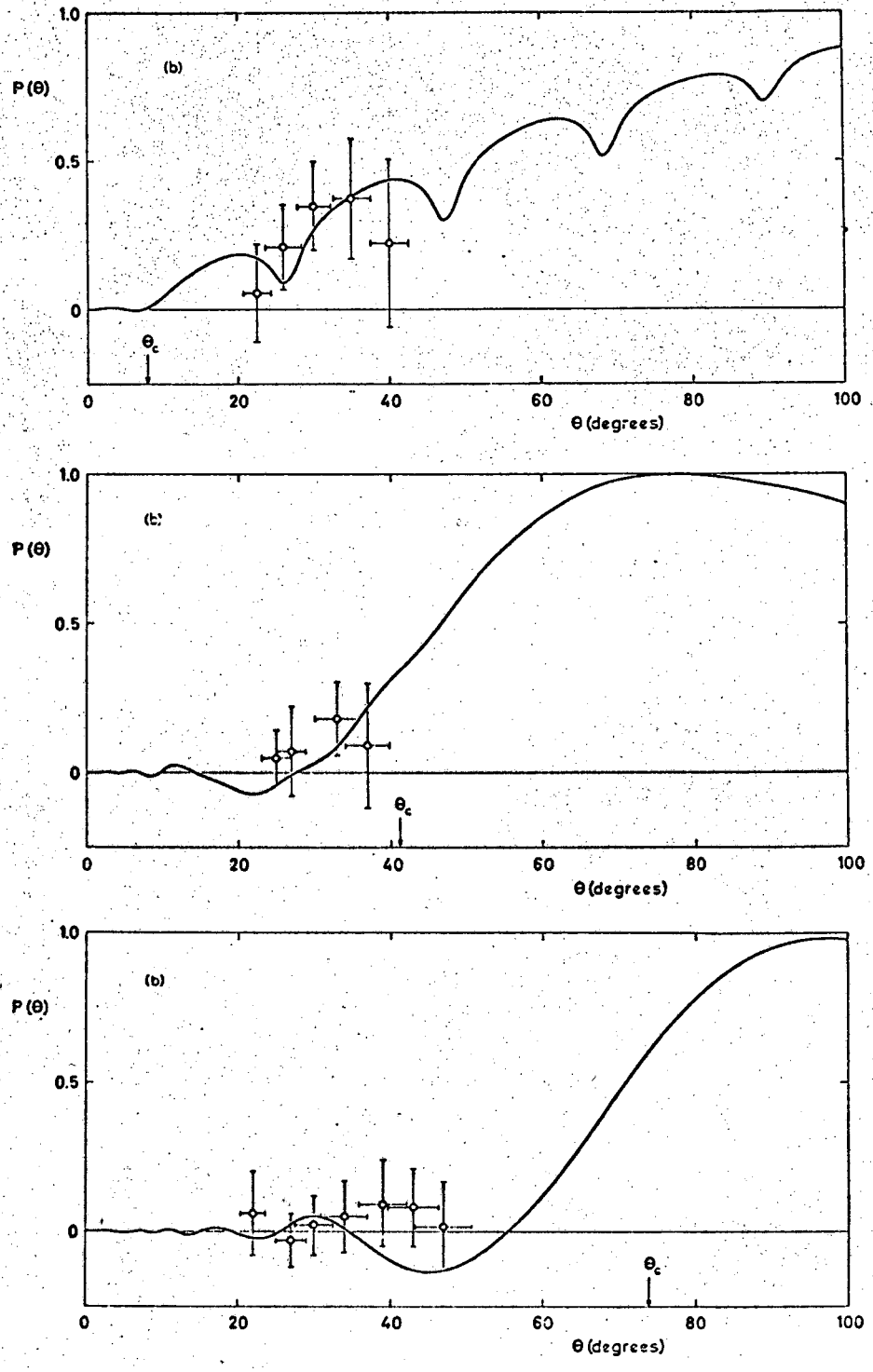

XBL 6711-6007

Fig. 7.

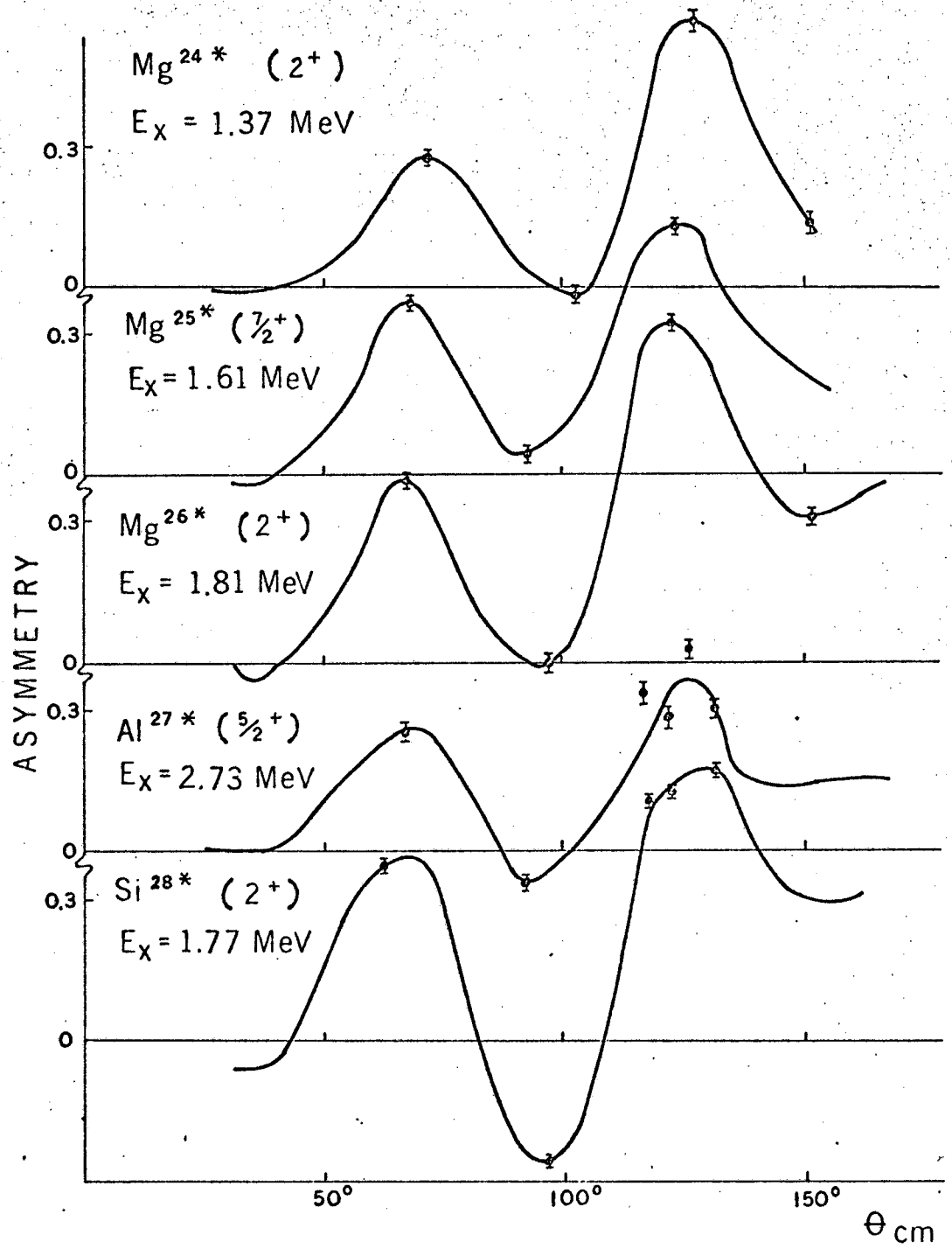

XBL 6711-6094

Fig. 8.

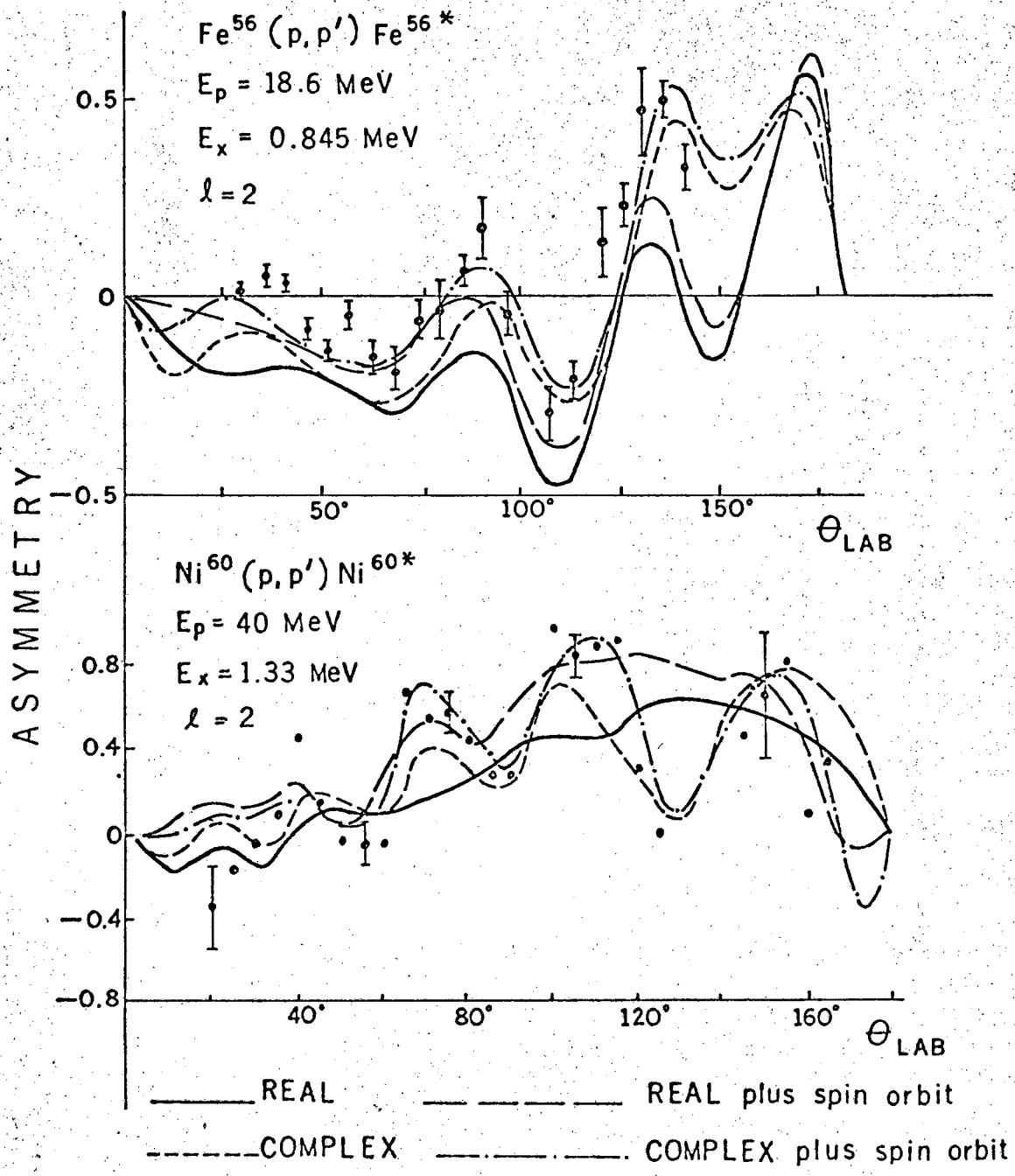
Fe56 (p, p') Fe56*
Ep = 18.6 MeV
Ex = 0.845 MeV
ℓ = 2
0.5
0
−0.5
50°
100°
150°
θLAB
Ni60 (p, p') Ni60*
Ep = 40 MeV
Ex = 1.33 MeV
ℓ = 2
0.8
0.4
0
−0.4
−0.8
40°
80°
120°
160°
θLAB
ASYMMETRY
REAL
REAL plus spin orbit
COMPLEX
COMPLEX plus spin orbit
XBL 6711-6095

Fig. 9.

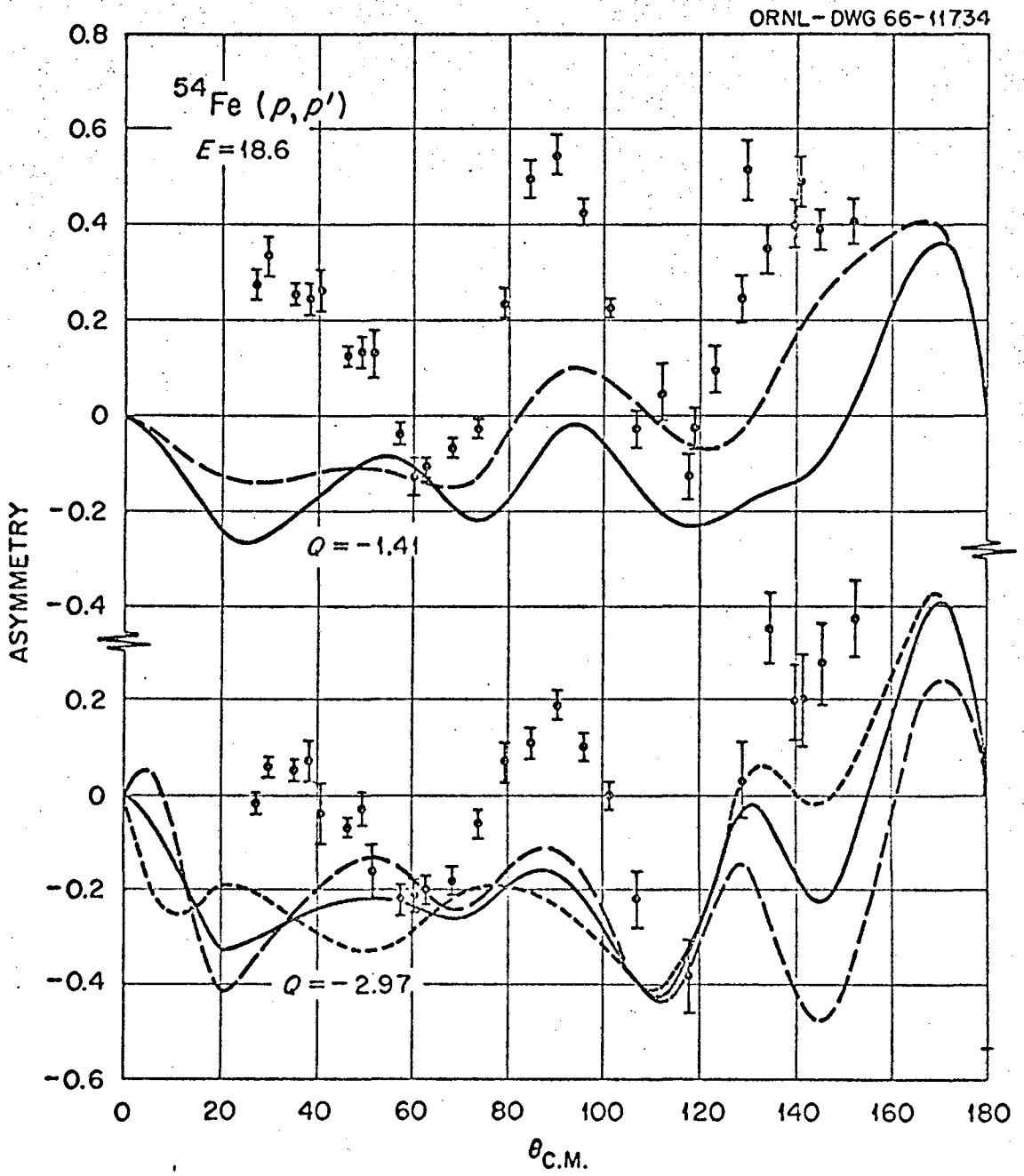

XBL 6711-6003

Fig. 10.

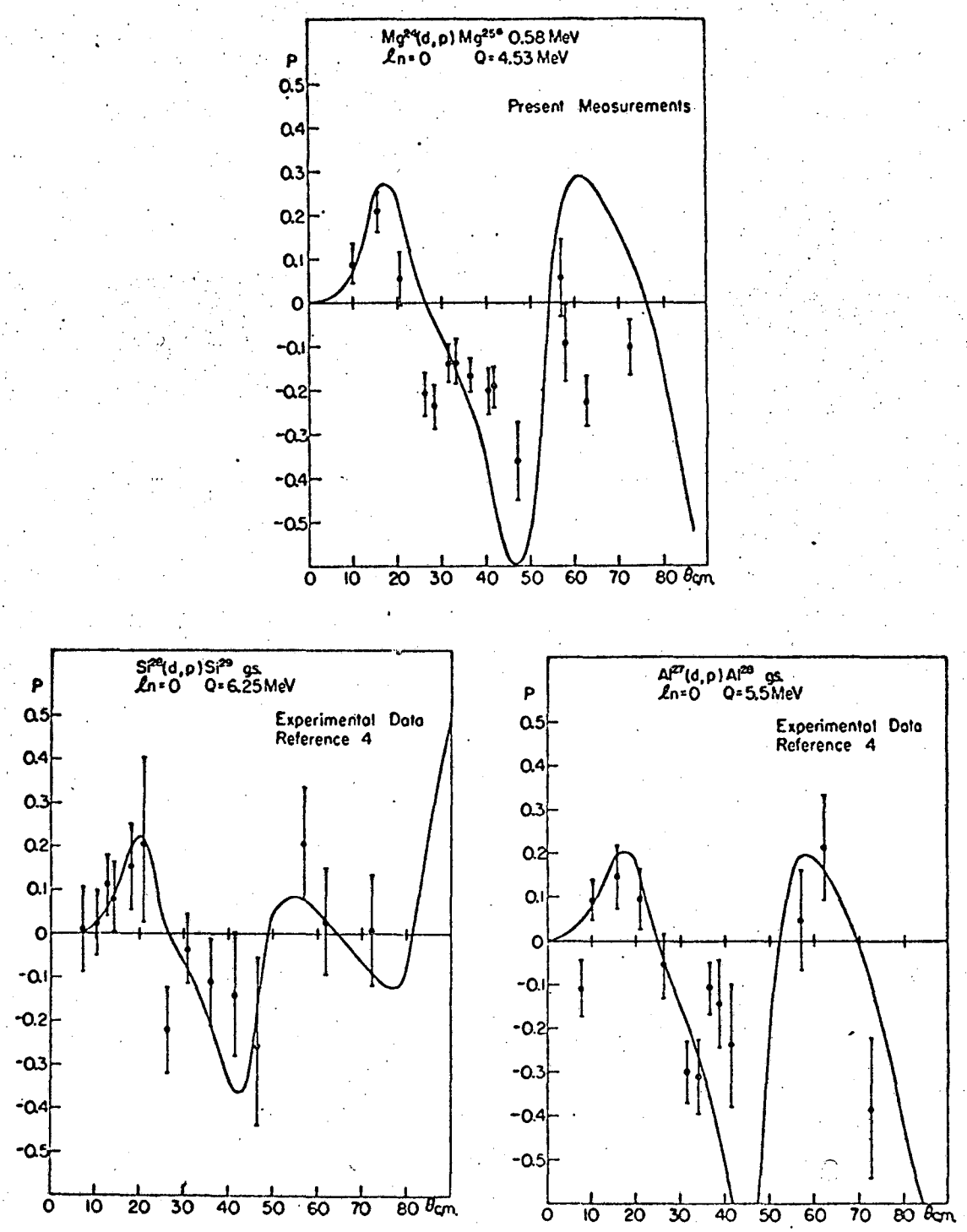
Mg²⁴(d,p) Mg²⁵* 0.58 MeV
ℓn = 0 Q = 4.53 MeV
Present Measurements
Si²⁸(d,p) Si²⁹ gs.
ℓn = 0 Q = 6.25 MeV
Experimental Data
Reference 4
Al²⁷(d,p) Al²⁸ gs.
ℓn = 0 Q = 5.5 MeV
Experimental Data
Reference 4
P
θcm
XBL 6711-6004

Fig. 11.

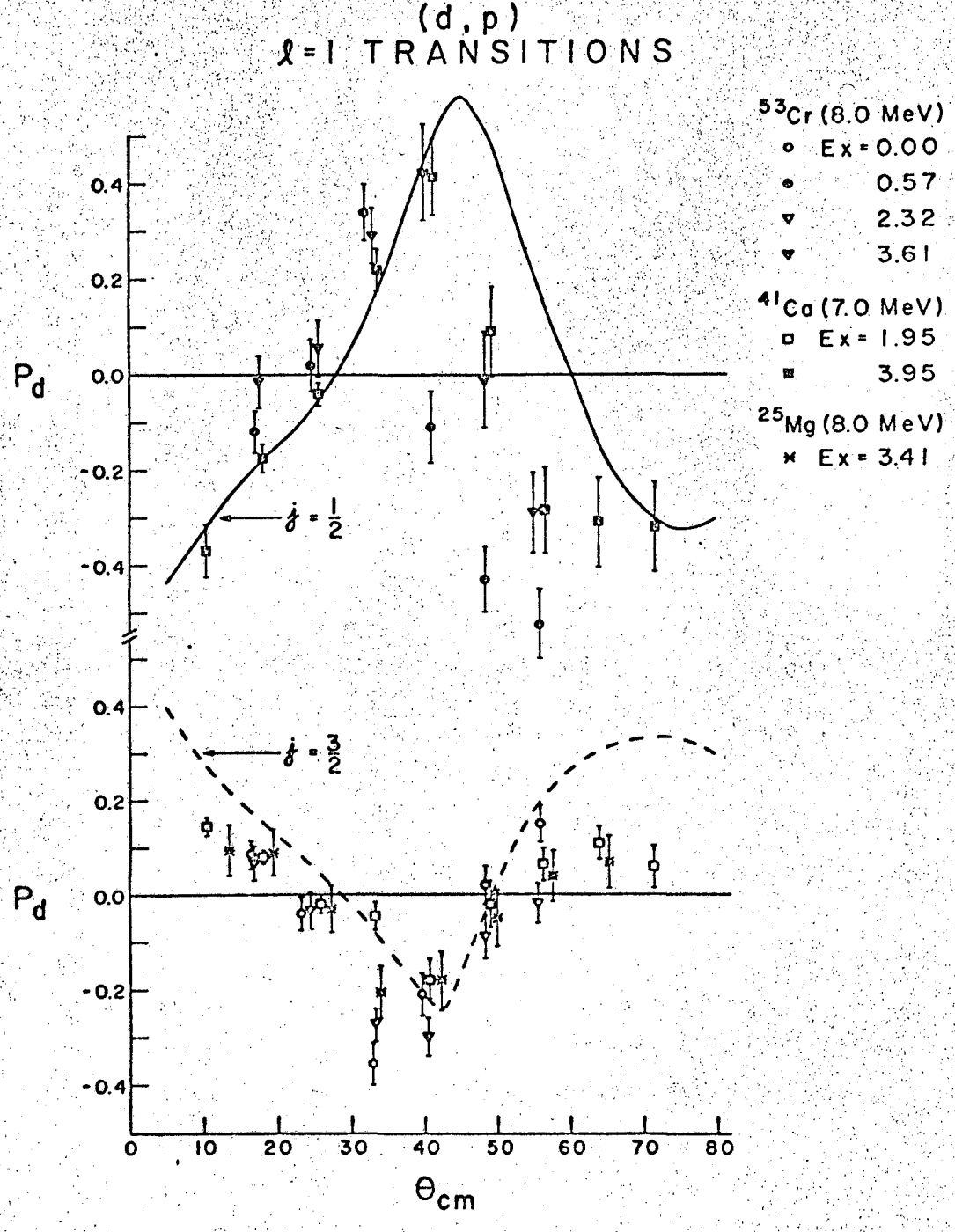
(d, p)
ℓ = 1 TRANSITIONS
^{53}Cr (8.0 MeV)
Ex = 0.00
0.57
2.32
3.61
^{41}Ca (7.0 MeV)
Ex = 1.95
3.95
^{25}Mg (8.0 MeV)
Ex = 3.41
P_d
$j = \frac{1}{2}$
$j = \frac{3}{2}$
0.4
0.2
0.0
-0.2
-0.4
0
10
20
30
40
50
60
70
80
Θ_{cm}
XBL 6711-6097

Fig. 12a.

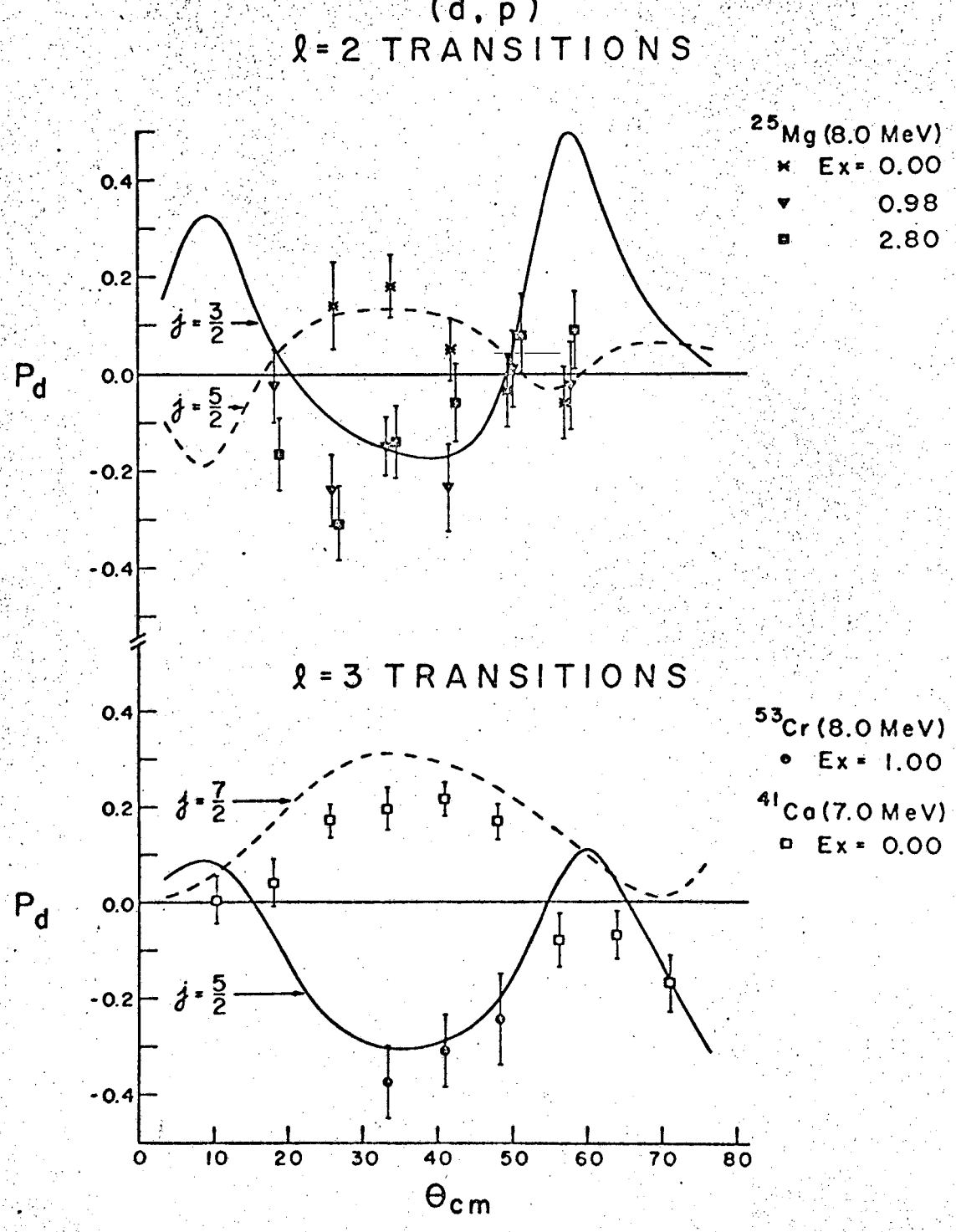

XBL 6711-6096

Fig. 12b.

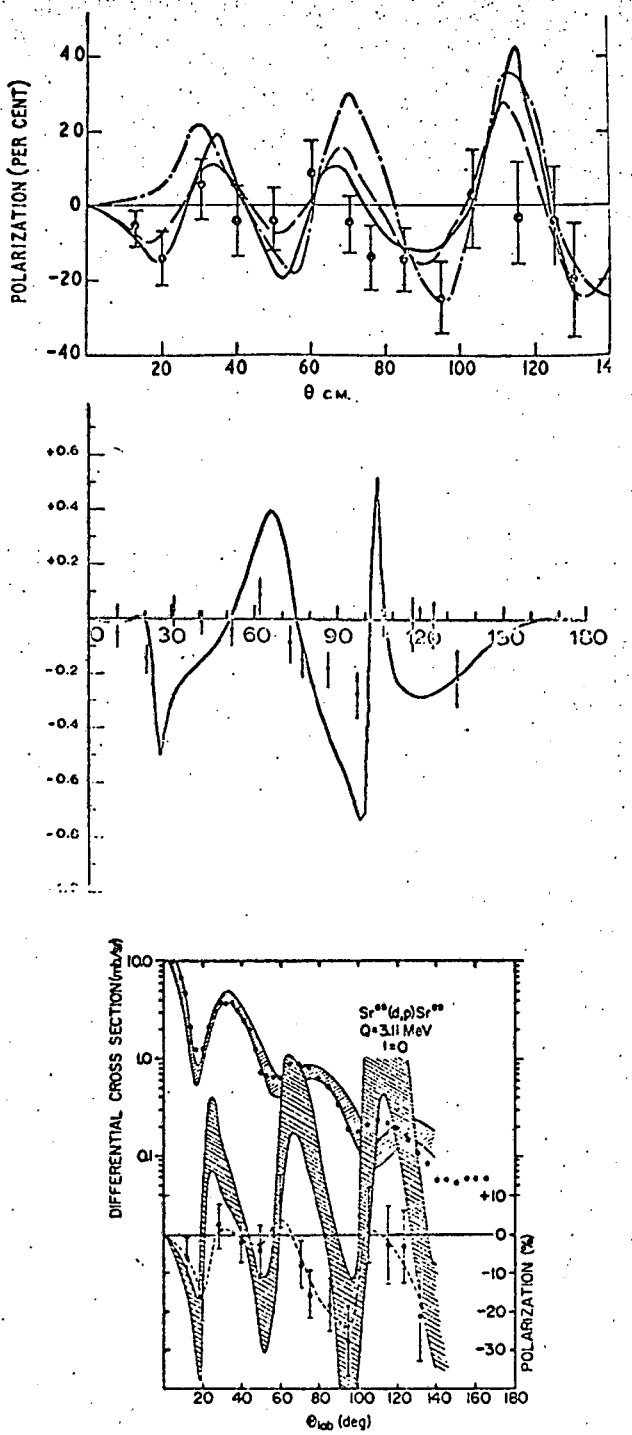

XBL 6711-6005

Fig. 13.

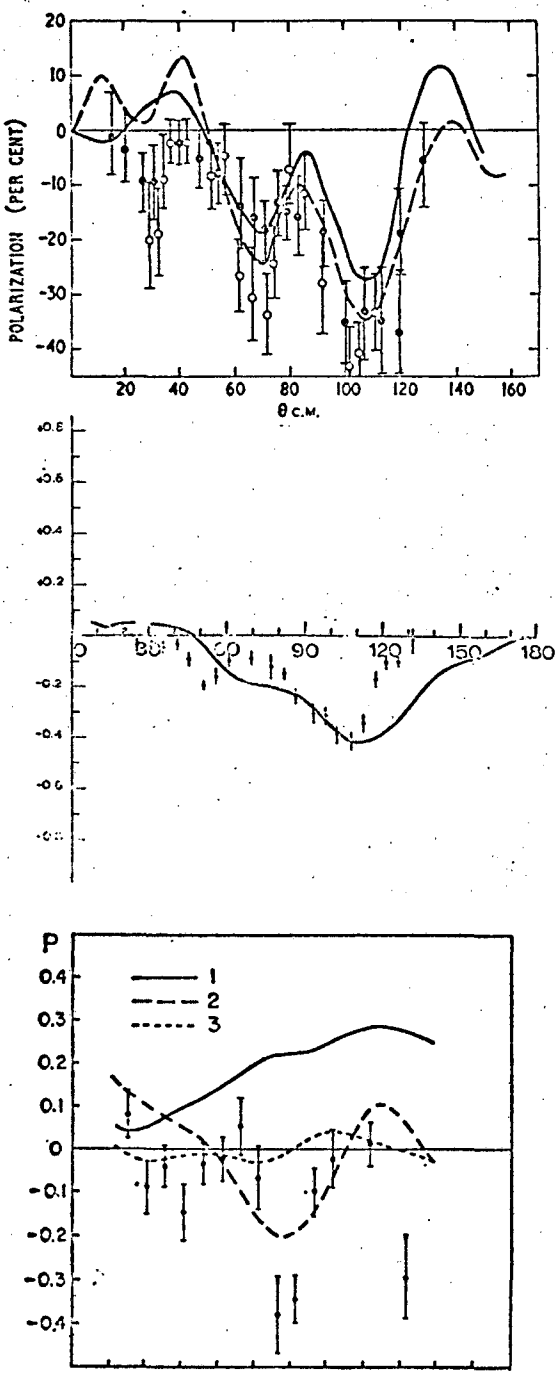

XBL 6711-6006

Fig. 14.